Exploring the link between star and planet formation with Ariel

Diego Turrini, Claudio Codella, Camilla Danielski, Davide Fedele, Sergio Fonte, Antonio Garufi, Mario Giuseppe Guarcello, Ravit Helled, Masahiro Ikoma, Mihkel Kama, Tadahiro Kimura, J. M. Diederik Kruijssen, Jesus Maldonado, Yamila Miguel, Sergio Molinari, Athanasia Nikolaou, Fabrizio Oliva, Olja Panić, Marco Pignatari, Linda Podio, Hans Rickman, Eugenio Schisano, Sho Shibata, Allona Vazan, Paulina Wolkenberg

Turrini D.
INAF - Osservatorio Astrofisico di Torino, Via Osservatorio 20, I-10025, Pino Torinese, Italy
Institute of Space Astrophysics and Planetology INAF-IAPS, Via Fosso del Cavaliere 100, I-00133, Rome, Italy, E-mail: diego.turrini@inaf.it

Fonte S., Schisano E., Molinari S., Oliva F., Wolkenberg P.
Institute of Space Astrophysics and Planetology INAF-IAPS, Via Fosso del Cavaliere 100, I-00133, Rome, Italy

Fedele D.
INAF - Osservatorio Astrofisico di Torino, Via Osservatorio 20, I-10025, Pino Torinese, Italy
INAF - Osservatorio Astrofisico di Arcetri, Largo E. Fermi 5, I-50127 Firenze, Italy

Codella C., Garufi A., Podio L.
INAF - Osservatorio Astrofisico di Arcetri, Largo E. Fermi 5, 50127 Firenze, Italy

Danielski C.
Instituto de Astrofísica de Andalucía (IAA-CSIC), Glorieta de la Astronomía s/n, 18008 Granada, Spain

Guarcello M. G., Maldonado J.
INAF - Osservatorio Astronomico di Palermo, Piazza del Parlamento 1, I-90134, Palermo, Italy

Helled R.
Institute for Computational Science, Center for Theoretical Astrophysics & Cosmology University of Zurich, CH-8057 Zurich, Switzerland

Ikoma M., Kimura T., Shibata S.
Department of Earth and Planetary Science, The University of Tokyo, 7-3-1 Hongo, Bunkyo-ku, Tokyo 113-0033, Japan

Kama M.
Department of Physics and Astronomy, University College London, London, WC1E 6BT,

Abstract The goal of the Ariel space mission is to observe a large and diversified population of transiting planets around a range of host star types to collect information on their atmospheric composition. The planetary bulk and atmospheric compositions bear the marks of the way the planets formed: Ariel's observations will therefore provide an unprecedented wealth of data to advance our understanding of planet formation in our Galaxy. A number of environmental and evolutionary factors, however, can affect the final atmospheric composition. Here we provide a concise overview of which factors and effects of the star and planet formation processes can shape the atmospheric compositions that will be observed by Ariel, and highlight how Ariel's characteristics make this mission optimally suited to address this very complex problem.

Keywords Ariel - Planet formation - Protoplanetary Discs - Star Formation - Galactic Environment - Stellar Characterization

1 Introduction

The study of the initial stages of the life of planetary systems, when planets are forming within the gaseous embrace of protoplanetary discs, has been undergo-

UK
Tartu Observatory, University of Tartu, Observatooriumi 1, 61602, Tõravere, Estonia

Kruijssen J. M. D.
Astronomisches Rechen-Institut, Zentrum für Astronomie der Universität Heidelberg, Mönchhofstraße 12-14, 69120 Heidelberg, Germany

Miguel Y.
Leiden Observatory, Leiden University, Niels Bohrweg 2, 2333CA Leiden, The Netherlands
SRON - Netherlands Institute for Space Research, Sorbonnelaan 2, NL-3584 CA Utrecht, The Netherlands

Panić O.
School of Physics and Astronomy, E. C. Stoner Building, University of Leeds, Leeds LS2 9JT, United Kingdom

Rickman H.
Centrum Badań Kosmicznykh Polskiej Akademii Nauk (CBK PAN), Bartycka 18A, 00-716 Warszawa, Poland

Pignatari M.
E.A. Milne Centre for Astrophysics, Department of Physics & Mathematics, University of Hull, HU6 7RX, United Kingdom
Konkoly Observatory, Research Centre for Astronomy and Earth Sciences, Hungarian Academy of Sciences, Konkoly Thege Miklos ut 15-17, H-1121 Budapest, Hungary
Joint Institute for Nuclear Astrophysics - Center for the Evolution of the Elements, USA
NuGrid Collaboration, www.nugridstars.org

Nikolaou A.
Sapienza University of Rome, Piazzale Aldo Moro 2, 00185, Italy
European Space Agency, ESRIN, ESA Φ-lab, Largo Galileo Galilei 1, 00044 Frascati, Italy

Vazan A.
Department of Natural Sciences and Astrophysics Research Center of the Open university (ARCO), The Open University of Israel, 4353701 Raanana, Israel.

ing a transformation in recent years. The improved resolution of observational facilities is allowing us to directly observe, for the first time, the gaps and rings in the gas and dust of protoplanetary discs that were the theoretically predicted signatures of the appearance of giant planets. These observations are being accompanied by improvements in the compositional characterisation of the discs themselves, allowing the first direct comparisons between the volatile budgets in protostellar objects and in the comets of our Solar System.

These advances have proceeded in parallel with the continuous growth of the known population of extrasolar planets, whose current size exceeds 4000 members and is allowing for population studies at the level of individual planets, of planetary systems as a whole, and of the link between stellar and planetary characteristics. The overall picture emerging from all these fields of study, while still incomplete, is nevertheless clearly indicating how the characteristics of each individual planet are uniquely sculpted by those of the environment in which it forms, in turn set by the star and its own formation process.

Ariel (Tinetti et al., 2018), the M4 mission of the European Space Agency deemed for launch in 2029, will characterise the composition of hundreds of exoplanetary atmospheres, proving us with an unprecedentedly large and diversified observational sample (Tinetti et al., 2018; Zingales et al., 2018; Turrini et al., 2018; Edwards et al., 2019). Ariel's observations will further revolutionize our view of the formation and evolution of both individual planets and planetary systems by systematically introducing a new dimension, their atmospheric composition, in the study of these subjects.

The insight on the link between the star formation process and the compositional build of planets will become an increasingly important piece of the puzzle of unveiling the nature of exoplanets over the coming years. The goal of this paper is therefore twofold. The first part (Sects. 2-5) aims to explore the environmental factors linked to the star formation process and the evolution of protoplanetary discs that can impact the final build of the exoplanets that Ariel will observe. At the beginning of Ariel's observational campaign these factors might represent a source of uncertainty in the interpretation of the atmospheric data (e.g. an unknown composition of the host star). By the end of the nominal mission, however, Ariel's rich and diverse exoplanetary sample will allow to shed light on the interplay between these environmental factors and the planet formation process.

The second part (Sects. 6-8), which builds upon the science cases devised in the previous phases of the mission (Tinetti et al., 2018; Turrini et al., 2018), aims to detail more closely the implications of the planet formation process for Ariel's observations. Specifically, Sect. 6 will discuss in detail the case of giant planets, which currently represent the bulk of Ariel's observational sample (Edwards et al., 2019), while Sect. 7 will move to smaller planetary sizes and masses, discussing the interplay between the capture of the nebular gas and the outgassing from the planetary interior in shaping their atmospheres as primary, secondary or mixed. Finally, Sect. 8 will review the information that can be extracted by the architectures of the planetary systems hosting the planets that Ariel will observe to provide dynamical context to the interpretation of Ariel's

atmospheric data. Because of the interdisciplinary nature of the discussion throughout this paper, each section and subsection will include one *coloured box* providing the associated *take-home message*, to help readers to identify and connect the key points for all specific subjects discussed.

2 Circumstellar Discs as the Birth Environment of Planets

The cores and atmospheres of planets are composed of protostellar dust, ices, and gas that have undergone physical and chemical interactions in planet-forming discs around newborn stars. To interpret the full range of planetary properties that Ariel will reveal, and to contribute to its list of science questions, it is therefore critical to have a firm foundation in this stage.

The formation of stars of mass up to several $M_\odot$ is accompanied by the emergence of a flattened expanse of material in Keplerian rotation around the star, called the protoplanetary disc. First signs of protoplanetary discs are present from the early infall stages when the star is accreting significantly (Class 0-I, Lada, 1987). Class 0 is the stage where the protostar is fully embedded in its parent envelope and rapidly gains its mass. In the Class I stage, the star has already accreted most of its mass. In both these stages, the disc is the channel for accretion onto the star from the surrounding envelope, but it only becomes observationally accessible in Class I stage. The most accessible phase, observationally, is the Class II phase where the star has accumulated its mass almost entirely, becomes directly visible and is no longer embedded in its parent envelope, leaving only the protoplanetary disc.

Across these stages, the disc is the channel for accretion onto the star from the surrounding envelope, and accretion may proceed up to several Myr on the pre-main sequence. Emerging evidence from the ALMA and VLA interferometers indicates that the *average* mass of discs arond Solar-like stars decreases from 10^{-1} $M_\odot$ at Class 0 to $10^{-1.5}$ $M_\odot$ and 10^{-2} $M_\odot$ at Class I and II, respectively (e.g. Tychoniec et al., 2018). In other words, the planet-forming mass reservoir drops from $100\,M_J$ to $\leq 10\,M_J$ (Jovian masses) when moving from embedded to easily observable discs. While the matter will be discussed in more detail later in the text, it is worth mentioning already here that these disc mass estimates suffer from a number of caveats mainly due to our poor knowledge of the dust opacity and the gas-to-dust mass ratio. The latter is often assumed to be similar to that of the interstellar medium (ISM), whose gas-to-dust mass ratio is estimated being 100:1 (Bohlin et al., 1978).

Discs extend up to a few hundred au, with several known cases extending over 500 au. The disc mass consists almost entirely of gas, so the hydrostatic pressure opposes the gravitational pull toward the plane of rotation and supports an extended vertical structure. The disc vertical struture is characterized in terms of the scale height, defined as $h_R = H/R$ with H being the height above the disc midplane in au, and R the distance from the star in au. H in turn is defined as the ratio between the local sound speed c_s and orbital angular velocity Ω. Typical values of h_R range between a few 10^{-2} to 0.1 depending

on the temperature profile, hence the sound speed, of the disc (e.g. D'Alessio et al., 2001; Armitage, 2009), though recent evidence shows that gas and small dust grains can reach scale height of 0.15-0.25 at R> 100 au (e.g. Avenhaus et al., 2018). While the gas and small grains can reach such altitudes, large dust grains settle fast onto the disc midplane as shown e.g., by the ALMA survey of edge-on discs (Villenave et al., 2020).

At the final stage, Class III, the star has typically already reached the main sequence, and can be surrounded by a debris disc (i.e. Vega-like stars, Dominik and Habing 2000). A debris disc is an extremely flat disc containing solids only, and rather than a disc it is geometrically better described as one or more rings or belts, analogous to our asteroid and Kuiper belts (Matthews et al., 2014). With the high sensitivity of ALMA, we are finding that the boundary between protoplanetary and debris discs is blurred (Miley et al., 2018), with some debris discs containing gas, although much less than typical protoplanetary discs (Péricaud et al., 2016), and protoplanetary discs showing evidence of dust production by collisional mechanisms as debris discs (Turrini et al., 2019).

Two main processes have been proposed as possible pathway for the formation of giant planets, the *core accretion* (also called nucleated instability) scenario and the *disc instability* scenario, with different implications for the disc environment associated with the birth of these planets. We briefly highlight the main characteristics of these two processes in the following, referring the readers to the recent reviews by Helled et al. (2014) and D'Angelo and Lissauer (2018) for more in-depth discussions.

In the disc instability scenario giant planets form as a result of a local gravitational instability in the circumstellar disc, which leads to the formation of a gravitationally bound object that collapses under its own self-gravity on timescales of the order of a few to a few tens of orbital periods. Disc instability may happen through Classes 0-I, when the disc is massive and more likely to be unstable. The condition for disc instability is satisfied for low values of the Toomre parameter

$$G_T = \frac{c_s \Omega}{\pi G \Sigma} < 1 \tag{1}$$

with G being the gravitational constant and Σ the gas surface density. Thus, for disc instability to occur the disc must be cold and massive, a condition that can be easily satisfied in the outer region of very young discs (roughly beyond a few tens of au). In Class II, and by the time the envelope is gone, it is likely that the disc has also had sufficient time to reach stability although, observationally, it is quite difficult to exclude the possibility that some of the massive discs with spiral structures seen in Class II may be undergoing disc instability.

In the core accretion scenario (further discussed in Sect. 6) the giant planets first form a planetary core by accumulation of solid material in the inner and denser regions of protoplanetary discs (within the first few tens of au), meanwhile acquiring a more or less extended gaseous envelope by capturing gas from the circumstellar disc. When the mass of this expanded atmosphere

becomes comparable with that of the planetary core, the gas becomes gravitationally unstable and triggers a runaway gas infall phase that causes a very rapid mass growth of the planet. The time required for the planetary core to grow and trigger the instability of its extended atmosphere can vary between a few 10^5-10^6 years, while the runaway gas accretion timescale is an order of magnitude faster, ranging between a few 10^4 years and a few 10^5 years. Due to its longer timescales nucleated instability can operate well into Class II, as the time required for the growth of the planetary core can easily exceeds the age of typical Class I sources.

Because of the wealth of observationally constrained parameters of discs in Class II phase, the information we possess on discs is mainly related to this class, with only a few examples which could qualify as representative of disc instability conditions.

2.1 Gas and solids in protoplanetary discs

Almost the entire gas mass of the disc is in the form of molecular hydrogen (H_2) and helium (He), with the next most abundant molecule being CO, with abundance of $\leq 10^{-4}$ with respect to H. Direct total H_2 gas mass measurements are not feasible because H_2 lacks a permanent dipole moment, which makes its rotational emission unobservably weak. The first vibrational level requires $\sim 6000\,\mathrm{K}$ to excite, so ro-vibrational emission only probes a thin, hot surface layer of the inner disc, same as the fluorescent emission of H_2 (Thi et al., 2001). Consequently the gas mass pursuit has focused on species such as CO and HD.

The *H_2 isotopologue, HD*, has a permanent dipole moment and rotational transitions in the far-infrared. Even accounting for isotope-selective chemistry, *HD can be assumed to have a fixed abundance relative to H_2 throughout almost the entire disc* (Trapman et al., 2017). The HD/H_2 ratio is determined by the local Galactic D/H ratio, which is $(2.0 \pm 0.1) \times 10^{-5}$ (Prodanović et al., 2010). Detecting the $J = 1$–0 line with the *Herschel* Space Observatory allowed Bergin et al. (2013) to estimate a total mass of 0.05 $M_\odot$ in the disc around TW Hya (0.8 $M_\odot$ star). Later estimates, using more strongly constrained physical-chemical models and additional information from the HD $J = 2$–1 transition, found $(0.075 \pm 0.015)\ M_\odot$ (Trapman et al., 2017). HD detections have also yielded mass estimates for two other T Tauri discs: DM Tau (0.65 $M_\odot$ star) with $(2.9 \pm 1.9) \times 10^{-2}\ M_\odot$, and GM Aur (1.1 $M_\odot$ star) with $(2.5 \pm 20.4) \times 10^{-2}\ M_\odot$ (McClure et al., 2016). The three measurements, with gas masses of 20-80 M_J, are consistent with a dust-to-gas mass ratio of 1:100 (Bohlin et al., 1978).

It is important to note that particularly massive and bright discs were specifically targeted in these observations. Kama et al. (2020) have recently analysed the upper limits on the HD $J = 1 - 0$ line flux of discs around intermediate mass stars putting a strong constraint on the gas mass of the disc around HD 163296, $M_{\mathrm{disc}} \leq 0.067\,M_\odot$. Comparing this with the masses of five

candidate protoplanets in this disc, they find a giant planet formation mass efficiency of $\gtrsim 10\,\%$ for present-day values. Because of the moderate energy of the low-level rotational lines (HD J=1, $E/k_B = 128.5\,$K), the HD-based mass estimates rely on the knowledge of the disc thermal structure. This can be estimated comparing multiple transitions of optically thick lines with thermo-chemical models. An ideal disc "thermometer" is the CO rotational ladder (e.g. Fedele et al., 2016). By fitting simultaneously the fluxes of the low-J HD and multiple CO transitions with thermo-chemical models it is possible to obtain robust constraints to both the temperature structure and total gas mass (Trapman et al., 2017).

CO is the second most abundant molecule after H_2, with an abundance of $\leq 10^{-4}$ with respect to H_2, and its rotational emission lines are readily detected in the millimetre. Historically, many of the gas mass measurements have relied on such CO observations in the past, for the lack of ability to detect more reliable tracers with pre-ALMA instruments. Such *measurements yield lower limits to the total gas mass reservoir*, as these bright *emission lines are* also *optically thick* and trace higher layers, and not the disc midplane where the bulk of the mass resides and planets form (Dartois et al., 2003). Another issue affecting CO is depletion due to freeze-out, as deep in the cold midplane CO readily freezes onto dust grains as soon as the temperature is below 20 K.

Emission from CO isotopologues is less optically thick, and in fact $C^{18}O$ and $C^{17}O$ are largely optically thin, making gas in the midplane accessible through millimetre observations. This method already yielded gas measurements with pre-ALMA instruments (Panić et al., 2008) and is currently widely used. An important limitation is still the CO freeze out, and other depletion mechanisms such as selective photodissociation, due to which the CO abundance may be decreased below the commonly assumed values, thereby rendering such mass estimates lower limits only (e.g. Dutrey et al., 1996; Ansdell et al., 2016; Miotello et al., 2016). Depending on the disc surface density, even the commonly used $C^{18}O$ lines can be optically thick in inner $\sim 10-20\,$au of the disc and the use of even rarer isotopologues is required. Recently, ALMA detected the rarest CO isotopologues $^{13}C^{18}O$ (Zhang et al., 2017) and $^{13}C^{17}O$ (Booth et al., 2019; Booth and Ilee, 2020).

It was long unclear whether unexpectedly low CO-based total disc mass estimates were due to an overall lower gas mass or a lack of CO molecules ("CO depletion"). Detailed physical-chemical models constrained by the continuum spectral energy distribution, multiple CO transitions and spatially resolved line maps, HD fluxes or upper limits, and other data have confirmed that **elemental C and O can have a wide range of gas-phase abundances, from nominal to two orders of magnitude depleted**, depending on the disc (Bruderer et al., 2012; Favre et al., 2013; Du et al., 2015; Kama et al., 2016b; Trapman et al., 2017).

It should be noted that a measurement of the total optically thin CO isotopologue line flux by itself only yields a lower limit on the disc gas mass. Multi-line and continuum data can provide some insight into whether it is the CO abundance or the total gas mass which is low (e,g, Favre et al., 2013; Kama et al., 2016b; Woitke et al., 2016; Du et al., 2017). Recently, the rarest stable CO isotopologue $^{13}C^{17}O$ has been detected in the disc HD 163296, yielding a gas mass of $0.3 M_\odot$, a few times higher than obtained with more abundant isotopologues (Booth et al., 2019). It is not yet clear whether the lower HD-based mass ($\leq 0.067\,M_\odot$, Kama et al. 2020) is due to an enhancement of volatile abundances or something else.

At the time of their formation, *discs inherit the dust-to-gas ratio from the molecular clouds*, and this fiducial value is often assumed to be 1:100 as measured in the ISM (Bohlin et al., 1978). *Measuring the dust mass is reliable to roughly an order of magnitude*, which is much better than the uncertainties linked to the gas mass estimates, except in the rare cases when HD emission is available as a constraint. The mass locked in dust grains of order a millimetre to centimetre in size is calculated directly from the observed flux at a wavelength similar to the grain size, assuming optically thin emission and a cold temperature ($\approx 20\,K$). For example, disc dust masses extend from 10^{-5} to $< 10^{-3}\,M_\odot$ in Lupus (Ansdell et al., 2016). The Lupus discs detected in CO lines typically have gas masses below $< 10^{-3}\,M_\odot$ (i.e., less than a Jovian mass of gas) which implies dust-to-gas ratios over 1:100.

As it has been recently shown, even at millimeter wavelength, the dust emission might not be optically thin throught the whole disc extent and self-scattering might bias the dust mass estimates that should be therefore considered as a lower limit (e.g. Zhu et al., 2019). As discussed above, the few available HD-based disc gas masses are in the 10 to $100\,M_{Jup}$ range. The field is currently trying to establish whether the low CO-based masses are real or a consequence of depletion of gas-phase elemental C and O (Krijt et al., 2018; Schwarz et al., 2018). Future observations at even longer wavelengths with e.g., the ngVLA, will help to better constrain the total dust mass (e.g., Isella et al., 2015). We expect substantial progress on understanding disc gas mass evolution and planet formation efficiency over the coming years, particularly by the time Ariel is due to fly.

Average dust masses derived from millimetre emission fail to reach $10\,M_\oplus$. This said, the dust mass just refers to the solid material presently in form of dust in the protoplanetary discs and *does not provide any indication of how much solid material is contained in form of rocks and larger bodies*. These contribute to a negligible fraction of the millimetre flux, dominated by the grains of comparable size to the wavelength. Dust mass measurements are improved by complementary measurements of the dust spectral index, which provides a better grasp of dust opacity - one of the key sources of uncertainty.

2.2 Chemical composition and molecular inventory of protoplanetary discs

Figure 1 summarises the inventory of molecules detected in discs (in the gas phase) at various wavelengths. Several carbon-, oxygen-, nitrogen- and sulphur-bearing species have been detected. Infrared observations of class II discs from the ground (with e.g., Keck/Nirspec and VLT/CRIRES) and from space (NASA/Spitzer and ESA/Herschel) revealed a molecule-rich inner disc. The most commonly detected species are OH and H_2O (e.g., Carr and Najita 2008; Mandell et al. 2008; Pontoppidan et al. 2010; Salyk et al. 2011; Fedele et al. 2011; Mandell et al. 2012; Fedele et al. 2012, 2013). CO rovibrational emission has been a particularly powerful tracer of the structure of the inner disc and geometry of disc cavities and gaps (e.g., Pontoppidan et al. 2008; Brittain et al. 2009; van der Plas et al. 2009; Salyk et al. 2011; Brown et al. 2013). A few simple organics molecules are also detected: HCN, C_2H_2 and CO_2 (e.g., Carr and Najita 2008; Pascucci et al. 2009; Pontoppidan et al. 2010; Salyk et al. 2011; Mandell et al. 2012) as well as CH_4 (seen in absorption in the disc around GV Tau N, Gibb and Horne 2013). These hot transitions emit from the inner ($\lesssim 10\,au$) warm molecular layer where molecules form primarily through gas-phase reactions (see e.g., Woitke et al. 2009; Walsh et al. 2015; Agúndez et al. 2018). A further contribution can come from the thermal desorption of the ices within the H_2O snowline. The large column density of OH and H_2O requires an oxygen-rich inner disc. On the contrary, at longer wavelength, deep Herschel/HIFI observations of the ground state rotational transitions of H_2O resulted in only 2 detections in the discs around TW Hya and HD 100546, while the lines remain largely undetected in other discs (Hogerheijde et al., 2011; Du et al., 2017) implying low abundance of cold H_2O ($\lesssim 10^{-11}$). The ground state H_2O emission is expected to come from the outer disc region ($> 50\,au$) where H_2O ice is photo-desorbed (e.g., Woitke et al., 2009). The emerging scenario is that, in the outer disc, oxygen is depleted onto icy grains, which release oxygen back to the gas-phase in the inner disc as they cross the water snowline, yielding an oxygen-rich inner disc (see also van Dishoeck et al., 2021)

Overall, the disc molecular inventory is made of a dozen of simple species. Complex molecules (i.e. composed of 6 or more atoms) are rare and the most complex species detected so far are: methanol (CH_3OH, Walsh et al. 2016), methyl cyanide (CH_3CN, Öberg et al. 2015) and formic acid (HCOOH, Favre et al. 2018). Recent observations of the FU Orionis-like object V883 Ori revealed the presence of more complex species such as CH_3CHO and CH_3COCH_3 along with CH_3OH (van 't Hoff et al., 2018; Lee et al., 2019b), opening the path to the investigation of complex species in discs. For most of the species, we do not have direct information of their radial and vertical distribution. Thanks to ALMA however, we are starting to spatially resolve the molecular emission, which informs us about the radial distribution of different volatiles.

Outer disc. On 10 to 100 au scales, spatially unresolved gas-phase total elemental abundances or abundance ratios are, thus far, available for carbon (C), oxygen (O), nitrogen (N), and sulfur (S). These abundances are typi-

Ionization	CH^+, $^{13}CH^+$, HCO^+, $H^{13}CO^+$, $HC^{18}O^+$, DCO^+, N_2H^+
Hydrogen	H_2, HD
Carbon	CO, ^{13}CO, $C^{18}O$, $^{13}C^{18}O$, $^{13}C^{17}O$, CO_2, C_2H, C_2D, C_2H_2, C_3H_2, CH_4
Oxygen	OH, H_2O, H_2CO, $HCOOH$
Nitrogen	CN, $C^{15}N$, HCN, $HC^{15}N$, $H^{13}CN$, DCN, HNC, DNC, NH_3, HC_3N
Sulphur	CS, ^{13}CS, $C^{34}S$, SO, SO_2, H_2S, H_2CS
Complex	CH_3CN, CH_3OH, CH_3CHO, CH_3OCHO, CH_3COCH_3

Fig. 1 List of molecules detected in protoplanetary discs at any wavelength. An increasing number of molecular isotopologues is being discovered at millimeter wavelenghts by ALMA. The detection of acetaldehyde (CH_3CHO), methyl formate ($CH_§3OCHO$) and acetone (CH_3COCH_3) refers to the outbursting source V883 Ori (van 't Hoff et al., 2018; Lee et al., 2019b).. The detection of C_3H_2 actually refers to c-C_3H_2, the cyclic form of this isomer whose linear form is yet to be detected in discs.

cally constrained by models including the disc physical structure, a chemical network, and ray-tracing of continuum and line emission. Sometimes, the vertically-integrated column density is the modelled quantity. In most cases, observational constraints include rotational lines of multiple species. The outer disc gas-phase elemental abundance and ratio measurements published to-date are summarized in Table 1.

Inner disc. On 0.1 to 10 au scales, in what was traditionally expected to be the formation zone of most planets before ALMA surveys revealed the possible signatures of giant planets at tens or even hundreds of au from the host stars (e.g. Andrews et al., 2018), elemental and chemical abundances are very hard to determine due to the small emitting area and the poorly known physical structure of these regions. New techniques are focusing on studying the composition of the material accreting onto the central star as a proxy of the inner disc:

1. Actively accretion-dominated photospheres of young stars above 1.4 $M_\odot$ (Jermyn and Kama, 2018). Disc accretion rates are sufficient to cover the entire photosphere on weekly timescales in these stars, whose radiative envelopes are mixed with the deeper layers very slowly. Photospheric abundances provide a measurement of the absolute dust depletion level in gaps or cavities in the inner disc (Kama et al., 2015). This technique will in the near future allow to study variations in the mutual ratios of many elements, including C, N, O, S, Si, Fe, Mg, Al, Ca, and Ti. A recent result of its application has been the determination that $(89 \pm 8)\%$ of all sulfur atoms in the inner few au of discs are locked in a refractory component, likely FeS (Kama et al., 2019), confirming the picture depicted by the data provided by the meteorites and minor bodies in the inner (e.g. Palme et al.,

Table 1 Gas-phase elemental abundances in discs on 10 to 100 au scales.

Object	C/H $(\times 10^{-4})$	C/O	N/O	S/H $(\times 10^{-5})$	References
Sun	2.69	0.55	0.16	1.32	
DM Tau	$0.2 \ldots 1.0$	> 1		$< 10^{-2}$	1,2,3
GM Aur	10^{-2}				1
GO Tau		> 1		$< 10^{-2}$	2
HD 100546	1.35	< 0.9		$*10^{-4}$	4
	0.135	< 0.9		$*10^{-3}$	5
IM Lup		0.8	10		6
LkCa 15		> 1		$< 10^{-2}$	2
TW Hya	0.01	> 1.1		$*10^{-4}$	5,7,8

Notes. Reported abundances with respect to H nuclei may have systematic uncertainties of a factor of a few. The difference between C/O < 1 and > 1 is strongly constrained and largely unrelated to these absolute scalings. *References*: 1: McClure et al. (2016); 2: Dutrey et al. (2011); 3: Semenov et al. (2018); 4: Kama et al. (2016a); 5: Kama et al. (2016b); 6: Cleeves et al. (2018); 7: Favre et al. (2013); 8: Trapman et al. (2017); *: upcoming publications.

2014; Lodders, 2019, and references therein) and outer (e.g. Altwegg et al., 2019; Rubin et al., 2020, and references therein) Solar System.

2. Atomic emission lines from the inner accretion disc where all dust has evaporated (Ardila et al., 2013). While these lines are hard to relate to absolute abundances, C and Si line emission can constrain major disc features such as the re-appearance of volatile carbon (reduced in outer disc gas by $\approx 50\times$) within the dust-depleted inner cavity in TW Hya (Kama et al., 2016b; McClure, 2019) or dust-evolution driven time variability in the inner disc volatile composition (Booth et al., 2017).

3 The Influence of the Stellar and Galactic Environments

Planetary systems do not form and exist in isolation, but instead are subject to radiative and dynamical influences from their cosmic environment. The birth of stars and planets takes place at local density peaks in the hierarchically structured ISM (e.g. Krumholz and McKee 2005; Kennicutt and Evans 2012). The fractal nature of the ISM causes star formation to be spatially clustered (e.g. Elmegreen and Falgarone, 1996; Kruijssen, 2012; Hopkins, 2013). In other words, planetary systems are often born and sometimes evolve in the vicinity of other stars and planetary systems, which can have an important impact on their properties (see Adams 2010 and Kruijssen and Longmore 2020 for recent reviews).

The two dominant, external physical mechanisms that are generally considered to affect the properties of planetary systems are:

1. *external photoevaporation* by massive stars, which accelerates the dispersal of protoplanetary discs and potentially modifies their chemistry and thermal structure, including the location of the snowlines (e.g. Scally and Clarke, 2001; Winter et al., 2018b);

2. *dynamical encounters* with other stars, which can perturb either the proto-
   planetary disc or, on longer timescales, disrupt the planetary system itself
   (e.g. Marzari and Picogna, 2013; Davies et al., 2014; Rosotti et al., 2014;
   Bhandare et al., 2016).

Observational indications of these mechanisms have been found. For instance,
observations show a variation of the protoplanetary disc size with ambient
stellar density (de Juan Ovelar et al., 2012), a variation of the protoplanetary
disc mass with distance to the nearest massive star (Ansdell et al., 2017),
a decline of the fraction of stars with discs in clusters at increasing values
of local UV fluxes (Guarcello et al., 2016), and tidal features as evidence
of past dynamical encounters between protoplanetary discs (Winter et al.,
2018a). It requires little imagination to realise that these effects can transform
the architecture of the resulting planetary systems, as well as affect the bulk
composition of the planets and that of their atmospheres.

It depends on the observable quantity of interest and on the timescale con-
sidered whether external photoevaporation or dynamical encounters dominate.
When only concerned with protoplanetary disc dispersal, external photoevap-
oration is almost always the dominant external mechanism, except in (rare)
cases of high stellar densities and no massive stars (Winter et al., 2018b,
2020a). However, in the context of Ariel, we are not only interested in the
truncation of the planet formation process, but also in the effect of external
photoevaporation and irradiation on planet formation through changes in the
chemistry and/or the thermal environment of discs. These processes require
much less extreme circumstances (e.g. radiation fields of a few 100 G_0, Ciesla
and Sandford 2012) than externally accelerated disc dispersal ($> 10^3$ G_0, Win-
ter et al., 2020a). For instance, the synthesis of complex organic molecules and
amino acids on icy dust grains is expected to be accelerated under external
UV or soft X-ray irradiation (e.g. Muñoz Caro et al., 2002; Throop, 2011;
Ciaravella et al., 2019). Likewise, the formation of planetesimals may be ac-
celerated by an external UV field (e.g. Shuping et al., 2003; Throop and Bally,
2005). For both of these examples, it is plausible that the effect of external UV
irradiation is a runaway process, because small dust grains can get trapped
in photoevaporative flows, causing a decrease of the extinction column and a
corresponding loss of UV absorption (e.g. Balog et al., 2006).

When concerned with the architecture of planetary systems over long
($\sim$Gyr) timescales, the expectation value for the number of disruption events
by dynamical encounters increases linearly with the age of the system, un-
der the assumption that the ambient environment does not evolve. Therefore,
eventually the integrated impact of dynamical encounters is expected to out-
weigh that of external photoevaporation and to become the dominant form of
external perturbation for older planetary systems. In this context, it is criti-
cal to consider the gravitational boundedness of the birth stellar population,
because only gravitationally bound clusters can generate sustained dynamical
perturbations – unbound stellar associations never live beyond a dynamical
crossing time (Gieles and Portegies Zwart, 2011), implying that encounters

are an extreme rarity. In the current solar neighbourhood, about 5–10% of stars are born in bound clusters (e.g. Lada and Lada, 2003), but this is expected to have been much larger in the past, with up to 50% of all stars and planetary systems with ages > 8 Gyr having been born in bound clusters and potentially having been exposed to extreme external disruption (e.g. Kruijssen, 2012; Longmore et al., 2014; Pfeffer et al., 2018). Notwithstanding these arguments, a sufficiently dense field star population can rival that of stellar clusters (e.g. towards galactic centres), such that even the field can generate a significant number of dynamical encounters over a sufficiently long timescale.

> The above discussion has a number of crucial implications for the Ariel target selection and, more generally, for studying the link between planetary composition and formation environment. Above all, the fact that **the stellar and galactic environment beyond the confines of a planetary system can affect its architecture, composition, chemistry, and atmospheric properties**, implies that the target selection should aim for a diversity of possible formation environments.

Major efforts are currently being undertaken to link the properties of planetary systems to their large-scale stellar environment, with promising results (e.g. Winter et al., 2020b; Kruijssen et al., 2020; Longmore et al., 2021; Chevance et al., 2021). These studies show that planetary system architectures and planetary properties (e.g. multiplicity, semi-major axis distribution, Hot Jupiter incidence, planet radius distributions and uniformity) exhibit intriguing environmental dependences, which can be isolated most clearly for host stellar ages of 1-4.5 Gyr (Winter et al., 2020b). While it is not yet possible to unambiguously relate the current environmental conditions to those of the formation environment, there exist statistical trends that can already greatly inform the target selection of Ariel.

Specifically, the ambient stellar density of planetary systems at birth sets the strength of the external UV field, as well as the rates of external photo-evaporation, dynamical encounters, and nearby supernovae, affecting isotopic abundance ratios (e.g. Fujimoto et al., 2018). The birth density greatly increases with gas pressure and therefore age (due to cosmic evolution, up to about ~ 8 Gyr ago, Kruijssen 2012; Adamo et al. 2015; Pfeffer et al. 2018; Winter et al. 2020a), which is likely to result in age trends of chemistry and atmospheric properties. Additionally, we may expect a trend with host stellar mass, because the impact of external radiative effects increases towards lower host stellar masses, due to lower binding energies and gas pressures of the protoplanetary discs (e.g. Haworth et al., 2018; Winter et al., 2020a). These trends are accessible by Ariel within the solar vicinity, due to the wide range of ages (and thus cosmic formation environments, see e.g. Ruiz-Lara et al. 2020) and host stellar masses of the local population of planetary systems.

The above line of reasoning leads to the following recommendation. In addition to the well-documented internal, secular processes governing the formation and evolution of planetary systems, the cosmic formation environment

is a major axis along which Ariel's planet sample should be expected to reveal new, surprising, and physically important trends. To realise this discovery potential, Ariel should aim to target a sufficiently large sample of planets around low-mass stars, with a wide range of ages from comparatively young (~ 1 Gyr) to older (> 5 Gyr), because older planetary systems around low-mass stars are predicted to be most strongly influenced by environmental effects. In addition to this general guideline, it is to be expected that the ongoing efforts aimed at characterising the formation environments of at least some of the known exoplanetary systems will bear fruit before the Ariel target selection has been finalised.

4 The Importance of Stellar Characterisation

Today we already know that planetary systems form around different types of stars, including low-mass stars like our Sun and more massive stars. Planets were found around both main sequence stars and evolved stars, and even around compact objects left from supernova explosions, like pulsars (Wolszczan and Frail, 1992). Thanks to Ariel we will gain new fundamental data on planets as they are today, but crucial properties related to their formation environments in the discs are long gone and cannot be observed anymore. On the other hand, part of this fundamental information is still available and preserved in the host stars.

4.1 Stellar host mass, type and metallicity: State of the Art from available observations

An important stellar property is its chemical composition. The iron abundance, expressed as [Fe/H] (the log number abundance of Fe/H relative to solar), is frequently used as a proxy for the metal content of the star. Already from the early studies of just four systems Gonzalez (1997) noted that giant planets tend to orbit around metal-rich stars. It is well established that the frequency of gas-giant planets (whose planetary mass $M_p > 30$ $M_\oplus$) correlates with the stellar metallicity (Santos et al., 2001; Fischer and Valenti, 2005; Sousa et al., 2008; Johnson et al., 2010). While the Sun and other nearby solar-type stars have [Fe/H] ~ 0, typical exoplanet host stars have [Fe/H] > 0.15. Data shows that the percentage of stars with detected Jupiter-like planets with orbital periods less than 4 yr rises with the iron abundance from less than 3% for the FGK stars with subsolar metallicity, up to 25% for stars with [Fe/H] $\geq +0.3$ dex (Fischer and Valenti, 2005). On average, the metallicity distribution of stars with giant planets is shifted by 0.24 dex relative to that of stars without planets.

In contrast to the giant Jupiter-mass planets, less massive planets (either more similar to Neptune or super-Earths) do not form preferentially in higher metallicity environments (Udry et al., 2006; Sousa et al., 2008; Ghezzi et al.,

2010; Mayor et al., 2011). Indeed, the median metallicity for solar-type stars hosting low-mass planets is close to -0.10 dex, and a significant number of low-mass planets are orbiting around stars with metallicities as low as -0.40 dex (Mayor et al., 2011). This observational result is usually explained within the framework of core-accretions models (e.g. Pollack et al., 1996; Rice and Armitage, 2003; Alibert et al., 2004) which assume that the timescale needed to form an icy/rocky core is largely dependent on the metal content of the protostellar cloud. In this way, in low-metal environments, the gas has already been depleted from the disc by the time the cores are massive enough to start a runaway accretion of gas. As a result, only low-mass planets can be formed. A possible correlation between planetary mass and stellar metallicity have been also suggested by Jenkins et al. (2017).

The correlation between planetary occurrence and metallicity observed in main sequence stars may not extend to giant stars, as several studies have found contradictory results (e.g. Pasquini et al., 2007; Ghezzi et al., 2010; Maldonado et al., 2013; Mortier et al., 2013; Jofré et al., 2015; Reffert et al., 2015). Several explanations have been put forward to explain the possible lack of a planet-metallicity correlation in evolved stars including the accretion of metal-rich material, higher-mass protoplanetary discs, and the formation of massive gas-giant planets by metal-independent mechanisms. Note that red giants are the result of the evolution of MS dwarfs with spectral types G5V-B8V (stellar masses between 0.9 and 4 $M_\odot$). High-mass stars are likely to harbour more massive protoplanetary discs (Alibert et al., 2011; Muzerolle et al., 2003; Natta et al., 2004; Mendigutía et al., 2011, 2012). Simulations of planet population synthesis (Alibert et al., 2011; Mordasini et al., 2012) show that giant planet formation can occur in low-metallicity (low dust-to-gas ratio) but high-mass protoplanetary discs. This effect depends on the mass of the disc. The minimum metallicity required to form a massive planet is lower for massive stars than for low-mass stars. In this scenario, the fact that giant stars with planets do not show the metal-rich signature could be explained by the more massive protoplanetary discs of their progenitors. Planets around evolved stars show some peculiarities with respect to the planets orbiting around main-sequence stars, like a lack of close-in planets or higher masses and eccentricities (e.g. Maldonado et al., 2013). There is also a strong dependence of giant planet occurrence on stellar mass: stars of ∼1.9 $M_\odot$ have the highest probability of hosting a giant planet (Reffert et al., 2015).

More observational evidence has been reported presenting correlations between planetary radius and host star metallicity (Buchhave et al., 2014; Schlaufman, 2015), as well as correlations between the eccentricity of planets versus metallicity (Adibekyan et al., 2013; Wilson et al., 2018). Although no clear correlations have been found between the stellar metallicity and the planetary semi-major axis, recent works discussed whether the stellar hosts of hot Jupiters (a < 0.1 au) show higher metallicities than stars with more distant planets. For example, Maldonado et al. (2018) shows that the metallicity distribution of stars with hot gas-giant planets is shifted by 0.08 dex with respect to that of stars with cool distant giants. The authors also noted a paucity of hot

Jupiters orbiting stars with metallicities below -0.10 dex, whilst cool Jupiters can be found around more metal-poor stars. Along these lines, Bashi et al. (2017) and Santos et al. (2017) suggest that stars hosting massive gas-giant planets show on average lower metallicities than the stars hosting planets with masses below 4–5 M_{Jup}. Finally, unlike gas-giant planet hosts, stars with brown dwarfs do not show metal enrichment (e.g. Ma and Ge, 2014) although Maldonado and Villaver (2017) found that stars with low-mass brown dwarfs tend to show higher metallicities than stars hosting more massive brown dwarfs.

> The emerging picture is one in which **different planet formation mechanisms may operate altogether and their relative efficiency changes with the mass of the substellar object that is formed**. For substellar objects with masses in the range from 30 $M_{\oplus}$ up to several Jupiter masses, high host star metallicities are found, suggesting that these planets are mainly formed by the core-accretion mechanism. More massive substellar objects do not tend to orbit preferentially around metal-rich stars and are likely to be formed by gravitational instability or gravoturbulent fragmentation (Schlaufman, 2018; Maldonado et al., 2019).

Most of the planet-host stars with low iron content belong to the thick disc population (Haywood, 2008; Adibekyan et al., 2012). Thin-disc stars rotate faster than the local standard of rest and show solar α-element abundances (Mg, Si, Ca, Ti). On the other hand, the thick disc is enriched in alpha elements and lags behind the local standard of rest (Reddy et al., 2003, 2006). It has been argued that to form a sufficiently massive core, the quantity that should be considered is the surface density of all condensible elements beyond the ice line (Mordasini et al., 2012), especially the elements O, Si, and Mg (Robinson et al., 2006; Gonzalez, 2009). In particular, Mg, and Si have condensation temperatures very similar to Fe (Lodders, 2003). It is therefore likely that stars with intermediate metallicity might compensate their lower metal content with other contributors to allow for planet formation to occur. Along these lines, Adibekyan et al. (2012) found that most of the planet-host stars with low Fe content are enhanced by α elements. This α-enhancement is a common property of most of metal-poor stars and is an effect of galactic chemical evolution, as most of the present Fe is made in thermonuclear supernovae while most of the α-elements like O or Si are made mostly in massive stars.

Regarding other chemical abundances besides Fe, planet-hosting stars are largely indistinguishable in their enrichment histories of refractory elements (e.g. Bodaghee et al., 2003; Gilli et al., 2006; Adibekyan et al., 2012), or show rather modest overabundances, with respect to other stars without planets. Volatile elements (C, O, Na, S, and Zn) are important in the chemistry of protoplanetary discs and planets. Stellar abundances can be difficult to estimate and high resolution data with high signal-to-noise are necessary to quantifying them. Spectral lines can be weak and blended, depending by the specific element, and cooler stars (T < 4500 K) in particular present molecular bands

that need a specific approach for treating elemental abundances. Interestingly, most volatiles show a decreasing trend of [X/Fe] with increasing [Fe/H], but the abundance trends for planet-hosting stars for volatile elements are similar to those for the comparison stars at the corresponding (high) values of [Fe/H] (e.g. Ecuvillon et al., 2004, 2006; Gonzalez, 2006; da Silva et al., 2011). More references can be found in Perryman (2018).

The abundance of lithium is an important diagnostic of stellar evolution. Several works have suggested that stars with planets tend to have less lithium than stars without. In particular, Israelian et al. (2004) found an excess Li depletion in planet-hosting stars with effective temperatures in the range 5600-5850 K, but no significant differences at higher temperatures. While this result has been confirmed by the majority of studies (e.g. Gonzalez, 2008; Gonzalez et al., 2010; Delgado Mena et al., 2014, 2015), other works have reported an absence of depletion for planet-hosting stars (e.g. Ghezzi et al., 2010; Ramírez et al., 2012). High Li abundance has also been reported in several rapidly rotating red giants that might be attributed to recent planet engulfment (e.g. Adamów et al., 2012, 2014; Nowak et al., 2013).

Beryllium, like lithium, is another tracer of the internal structure and (pre) main-sequence evolution. A higher beryllium depletion has been found for stars with effective temperatures lower than 5500 K, but this process seems to be independent of the presence of planets (Delgado Mena et al., 2012). Detailed chemical abundances of planet hosts has shown that the Sun and other solar analogues are depleted on refractory relative to volatile elements by $\sim$0.08 dex when compared with the majority of nearby solar twins (e.g. Meléndez et al., 2009; Ramírez et al., 2009, 2010, 2014; Gonzalez et al., 2010; Gonzalez, 2011). After discussing several possible origins, Meléndez et al. (2009) conclude that the most likely explanation is related to the formation of planetary systems like our own, in particular to the formation of rocky low-mass planets. Although appealing, this hypothesis has been questioned, and other works point towards chemical evolution effects (González Hernández et al., 2010, 2013; Schuler et al., 2011; Maldonado et al., 2015), or an inner Galactic origin of the planet hosts (e.g. Adibekyan et al., 2014; Maldonado and Villaver, 2016) as their possible causes.

One aspect that is currently challenging the detection of low-mass planets is stellar activity (e.g. Dumusque et al., 2012). Exoplanet host stars display a wide variety of chromospheric and magnetic activities dependent mostly on their spectral type (e.g. Perryman, 2018, and references therein). For example, Isaacson and Fischer (2010) and Arriagada (2011) performed a detailed study of large samples of stars in planet search programs, using activity indexes to estimate the level of radial velocity jitter of the program stars. Canto Martins et al. (2011) compared the activity index R'_{HK} measured in stars with and without planets finding similar distributions. In addition, no significant correlations between R'_{HK} and the planetary properties were found. Gonzalez (2011) found that stars with planets have significantly smaller values of $v\sin i$ and R'_{HK} compared to otherwise similar non-planet hosts. No differences in the X-ray emission between planet hosts and non-host were found by Kashyap
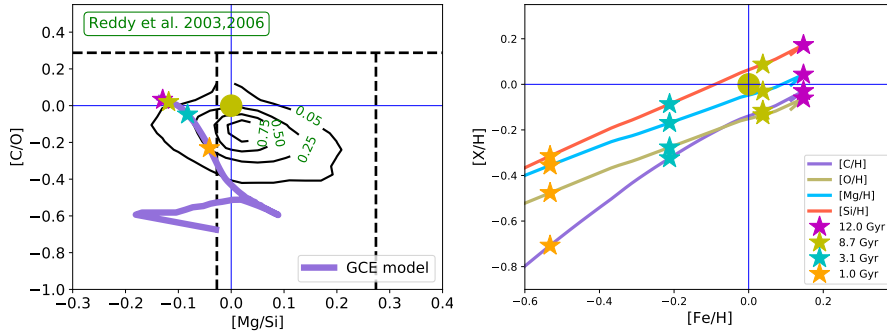
Fig. 2 *Left Panel:* stellar statistics distribution with respect to [C/O] and [Mg/Si] from observations Reddy et al. (2003, 2006) and GCE models. The elemental ratios are reported in logarithmic notation, scaled to solar value. The Sun is reported as reference, with blue lines indicating the solar ratios. Dashed black lines indicate the element classification relevant for planet behavior according to Bond et al. (2010). GCE simulations are reported (magenta line), with reference time symbols at 1 Gyr, 3.1 Gyr, 8.2 Gyr (which corresponds to the age of the Sun) and 12 Gyr after the formation of the Milky Way (orange, cyan, yellow and magenta star, respectively). *Right Panel:* [C/H], [O/H], [Mg/H] and [Si/H] are reported with respect to [Fe/H] for the same GCE model reported in the left panel.

et al. (2008) although the authors reported higher X-ray luminosities for the stars hosting close-in giant planets. However, Poppenhaeger et al. (2010) found no correlation between the X-ray luminosity and the planet's mass or orbital distance.

Observations indicate that host stars of some close-in hot Jupiters undergo episodes of periodic or enhanced stellar activity, linked to the presence of the planet through magnetic or tidal interactions (see e.g. Perryman, 2018, and references therein). Periodic activity has been reported both in the Ca II H & K and/or Balmer line emission in several planet-hosting stars, such as ν And and HD 179949, and inferred from optical brightness variations in the case of τ Boo (Scandariato et al., 2013; Shkolnik et al., 2005; Walker et al., 2008). Another example is HD 17156, where enhanced chromospheric and coronal emissions were detected a few hours after the passage of the planet at the periastron (Maggio et al., 2015).

4.2 Pristine chemical composition of the star and planet system

The original chemical composition of a stellar system, encompassing the star and its circumstellar disc, is part of the initial conditions for the planet formation process and sets some of the fundamental properties of the planets that the star will host. In particular, the initial chemical setup of the system will affect the envelope/mantle properties and the atmospheric composition of the planets. The relative ratios of elements such as O, C, Mg and Si will

set the mineralogy of the planets and the impact of volcanic activity on their atmospheres (e.g., Bond et al., 2010; Delgado Mena et al., 2010).

The information on the initial chemical composition of the system will be modified and partly erased throughout the planet formation process (e.g. due to the different behaviour of volatile and refractory elements and the effects of planetary migration, see Sects. 6 and 7). The surface/photospheric composition of the host star, however, will preserve this information almost unchanged over time (e.g., Piersanti et al., 2007). The characterization of the stellar composition, therefore, provides fundamental information and the context to reconstruct the dynamical and formation histories of planets from their observed atmospheric composition (see also Sect. 6). While the definition of the Solar System abundances (both present and protosolar) is constantly updated thanks to photospheric and meteoritic data, and today we know them with good precision (though uncertainties still remain, see e.g. the oxygen crisis, Palme et al., 2014; Lodders, 2019, and references therein), the same is not true for all stars.

> For most stars many elements are either not available or observed with much larger errors than Fe, and other elements like phosphorus and chlorine are not observable. Furthermore, the Milky Way disc is a complex system, where galactic chemical evolution (GCE) is changing chemical abundances over a timescale of billions of years, and the chemical enrichment history among stars with similar age and/or galactic location may show significant variations beyond observational errors. For this very reason, **the solar initial composition cannot be universally applied to different stellar systems**.

The characterization of the stellar host composition and of the initial planetary system composition needs to adopt a multi-disciplinary approach: available elemental spectroscopic data can be integrated with theoretical GCE simulations. In figure 2, left panel, the elemental ratios [C/O] and [Mg/Si] are shown for a stellar sample of the Milky Way disc by Reddy et al. (2003, 2006), covering a metallicity range similar to that of the Ariel expected targets (Edwards et al., 2019). The Sun is also reported for comparison. Without considering 5% of disc stars with more exotic composition, the remaining 95% stars show a variation of [C/O] and [Mg/Si] between 0.3 and 0.4 dex in logarithmic notation, which corresponds to a variation between a factor of 2 and 2.5. GCE simulations for one possible chemical enrichment history are also shown in Fig. 2 for comparison.

The model was generated using the GCE code OMEGA from the NuPyCEE package (Ritter and Côté, 2016; Côté et al., 2017). The yellow star symbol corresponds to the Sun formation time, 4.6 billions years ago. The model shown seems to provide an acceptable representation of the Sun, with a perfect match of the [C/O] ratio, and underestimating by about 0.1 dex (this corresponds to 25%) the [Mg/Si] ratio. The chemical enrichment history from the same model is shown in Fig. 2, right panel, for C, O, Mg and Si, in the relevant metal-

licity range [Fe/H] currently foreseen for the Ariel sample (Edwards et al., 2019). Within the metallicity range considered, it is interesting to observe the different trend of Si and C compared to O and Mg. This is due to the different chemical enrichment history of these elements (e.g., Timmes et al., 1995b; Kobayashi et al., 2011; Mishenina et al., 2017).

For a benchmark of the correct initial composition of all Ariel targets, an extended set of consistent GCE models will need to be generated covering the observations for element ratios like [C/O] and [Mg/Si], at the correct age of the stellar hosts. These models will have all the elements available, at any time, to compare with stellar observations and inform theoretical planet simulations. The relative abundance scatter obtained from these simulations need to be simulated, and their impact on planet simulations is still unknown.

4.3 Pristine radioactivity, local enrichment and galactic chemical evolution

Together with stable isotopes and elements, stars also make radioactive isotopes. Some of them have an half-life long enough to affect the formation and evolution of new-forming planetary systems. The ^{26}Al and ^{60}Fe isotopes have a half-life of 7.17×10^5 years and 2.62×10^6 years, respectively. Traces of extinct ^{26}Al and ^{60}Fe were found in the early Solar System condensates, and we know that their heat contribution is crucial during planetesimal formation (Lugaro et al., 2018, and references therein). The short half-life of ^{26}Al and its abundance derived from early Solar System material exclude a relevant GCE contribution. Therefore, its abundance in the protosolar nebula is due to the contribution of local stellar sources, like the explosion of nearby supernovae, baking these species relatively nearby and shortly before the formation of the Sun. The argument is more controversial for ^{60}Fe, where its low abundance relative to ^{26}Al in the early Solar System is making unclear if its composition was a GCE product or if it was dominated from local stellar sources, as for ^{26}Al (Côté et al., 2019b, and references therein).

Today we have evidence that pollution of radioactive material from other stars continued over time, not only during the formation of the Solar System. For instance, traces of the radioactive isotope ^{60}Fe have been discovered in fresh Antarctic snow, signifying further pollution from recent supernovae (Koll et al., 2019). Extinct ^{60}Fe has been detected in the ocean crust, falling through Earth's atmosphere and oceans about 2.2 million years ago (e.g., Ludwig et al., 2016). This has been connected with a mass extinction event affecting many species in our oceans about 2.6 million years ago, due to the radiation from the same nearby supernova (e.g., Melott et al., 2019). This makes really hard to define what is the correct amount of ^{26}Al and ^{60}Fe to use in simulations of planet formation.

Values obtained from meteorites for the early Solar System are the outcome of local stellar pollution or, perhaps, the combined outcome of stellar pollution and GCE for ^{60}Fe. Even an ideal stellar system, composed by a solar twin with the exact same elemental composition, may have a complete differ-

ent concentration of initial ^{26}Al and ^{60}Fe. And, as we mentioned before, GCE simulations alone are not providing a correct answer, since the half-life of these isotopes is too short. In preparation to Ariel's observations, a new generation of theoretical simulations will be needed. The initial ^{26}Al and ^{60}Fe abundances need to to be varied within a realistic range, from background GCE concentrations (e.g., Côté et al., 2019b), up to realistic abundances guided from stellar simulations of different types of stars that can produce ^{26}Al and ^{60}Fe (e.g., Timmes et al., 1995a; Limongi and Chieffi, 2006; Jones et al., 2019; Côté et al., 2019c).

The radioactive isotopes ^{40}K, ^{232}Th, ^{235}U and ^{238}U all have half-lifes of the order of 1 billion years or larger. Therefore, their galactic enrichment history behaves more like that of stable isotopes, and GCE simulations are needed to calculate their evolution in the interstellar medium. Once the planets are formed, the abundance of these species determines their internal heating history, sustaining tectonic activity and the magnetic field. The potassium observed today on the surface of the stellar host does not tell much about the initial ^{40}K, and thorium and uranium are extremely hard to observe in stellar spectra. A possible strategy would be to get the realistic range of these abundances from GCE simulations, where the stellar sources of these isotopes are properly considered.

This analysis is more difficult for thorium and uranium, since they are product of the rapid neutron capture process (r-process). The dominant astrophysical source of the r-process is still matter of debate, and several sites like neutron-star mergers have been proposed (e.g., Cowan et al., 2019; Côté et al., 2019a, and references therein). An approach complementary to the one mentioned above is to perform a study of the production of ^{40}K and actinide elements, to define observations from the abundance pattern measured in the stellar host that can be used as a diagnostic of their concentration. For instance, the r-process element europium measured from the surface of the stellar hosts could be used as a diagnostic for the initial abundance of the radioactive isotopes ^{232}Th, ^{235}U and ^{238}U. At present, there is no available estimation of how much the abundances of these isotopes may change in the galactic disc in the metallicity range of interest for Ariel targets.

5 Organics as C-O-N Carriers

In the last 10 years there has been a number of surveys dedicated to assess the molecular content of protoplanetary discs, targeting mostly the simpler bi- and tri-atomic molecules such as CO, CN, H_2O, HCO^+, DCO^+, N_2H^+, HCN, DCN (e.g. Fedele et al., 2013; Guilloteau et al., 2013, 2016; Öberg et al., 2010, 2011; Podio et al., 2013), as well as a few S-bearing species, e.g. CS, H_2CS, H_2S (e.g., Phuong et al., 2018; Teague et al., 2018; Le Gal et al., 2019; Codella et al., 2020; Garufi et al., 2020b,a; Loomis et al., 2020; van't Hoff et al., 2020). The content of complex organic molecules (COMs), on the contrary, is still only poorly known because of their lower gas-phase abundances ($< 10^{-8}$ with

respect to the abundance of atomic hydrogen). According to disc models this is due to the fact that COMs are frozen on the icy mantles of dust grains in the cold disc interior and only a tiny fraction of them is released in gas-phase through thermal or photo-/CR- desorption (e.g. Aikawa and Herbst, 1999; Willacy and Woods, 2009; Walsh et al., 2014; Loomis et al., 2015). Hence, (complex) organic molecules in protoplanetary discs remain hidden in their ices and can be unveiled only through interferometric observations at high sensitivity and resolution, e.g. with ALMA.

> The study of COMs in protoplanetary discs is key to estimate the fraction of C, O, and N atoms that are trapped in organic molecules. While it is generally thought that most of these atoms are incorporated in ices (in the form of, e.g. H_2O, CO_2, CO, etc), there is the possibility that organic molecules trap a significant amount of them, as also suggested by recent observations of comets in the Solar System (e.g. Fulle et al., 2019). **As organic molecules are carriers of C, O, and N, it is crucial to estimate their abundance and the location of their snowlines, to infer accurate C/O/N ratios in the gas and solids of discs, with direct implications for the final C/O/N ratios of planets**.

Thanks to ALMA a few simple organics have been imaged in discs. Among those, formaldehyde (H_2CO) and methanol (CH_3OH) are key to investigate organics formation. While H_2CO can form both in gas-phase and on grains, CH_3OH forms exclusively on grains. An illustrative example are the resolved ALMA images of H_2CO in nearby protoplanetary discs (Qi et al., 2013; Loomis et al., 2015; Öberg et al., 2017; Carney et al., 2017, 2019; Podio et al., 2019; Garufi et al., 2020b; Pegues et al., 2020; Podio et al., 2020a,b; Garufi et al., 2020a). These allowed us to infer the H_2CO abundance and distribution in protoplanetary discs and to constrain the mechanism(s) for its formation in this environment. This is key, given that H_2CO is one of the bricks for the formation of complex organic and prebiotic molecules.

The distribution of H_2CO suggests that the bulk of the observed H_2CO in the disc is formed via gas-phase reactions. This is indicated both by the o/p ratios measured in TW Hya (Terwisscha van Scheltinga et al., 2021) and by the vertical distribution of molecular emission in the edge-on disc of IRAS 04302 where H_2CO mostly arises from an intermediate disc layer, the so called molecular layer (Podio et al., 2020b; van't Hoff et al., 2020). However, for IRAS 04302 H_2CO emission is detected also in the outer disc midplane, where molecules are expected to be frozen onto the dust grain icy mantles. Also for a few discs the observations show a secondary emission peak of H_2CO located outside the CO snowline which may argue in favour of H_2CO formation on grains in these outer disc regions, following freeze-out of CO and its subsequent hydrogenation on the icy grains (Öberg et al., 2017; Carney et al., 2017; Podio et al., 2019; Pegues et al., 2020) (see e.g. Fig. 3-Right). This may indicate that ice chemistry is efficient in the outer regions of discs and could produce
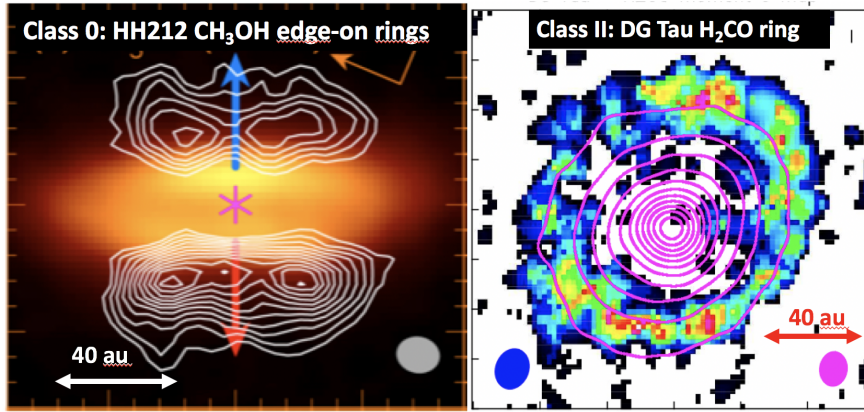
Fig. 3 The protostellar discs around the Class 0 star HH 212 and the protoplanetary disc of the Class II star DG Tau as observed with ALMA. *Left*: continuum (colour) and CH_3CO (contours) of the protostellar discs around HH 212. *Right*: continuum (contours) and H_2CO (colour) of the protoplanetary disc of DG Tau. Figures adapted from Lee et al. (2019a) and Podio et al. (2019).

methanol as well as other complex organics, which are then partly released in gas-phase via non-thermal processes. However, only a few of them has been so far detected, i.e. cyanoacetylene and methyl cyanide (HC_3N, CH_3CN, Öberg et al. 2015; Bergner et al. 2018), methanol (CH_3OH, Walsh et al. 2016; Podio et al. 2020a), and formic acid (HCOOH, Favre et al. 2018). Typical abundances are: 10^{-12}-10^{-10} (H_2CO), 10^{-12}-10^{-11} (CH_3OH, HCOOH, HC_3N), 10^{-13}-10^{-12} (CH_3CN).

At the protostellar stage observations are hindered by the presence of many kinematical components that may hide the chemical content of the disc, e.g. the surrounding envelope and the outflow. To date only one protostellar disc has been chemically characterised on Solar System scale, the disc of HH 212 (see Fig. 3-Left). This pioneering work shows enriched chemistry associated with the disc surface layers, with the detection of a number of complex organic molecules, e.g. CH_3OH (10^{-7}), HCOOH (10^{-9}), CH_3CHO (10^{-9}), $HCOOCH_3$ (10^{-9}), NH_2CHO (10^{-10}) (e.g. Codella et al., 2018, 2019; Lee et al., 2017, 2019a). These abundances are larger than what observed at the protoplanetary stage.

This chemical enrichment may be due to slow shocks occurring at the interface between the infalling envelope and the forming disc (e.g. Sakai et al., 2014). The chemically enriched gas should then settle in the rotationally-supported disc, where the chemical composition is likely stratified and affected by the dynamics and the dust coagulation. The scenario obtained for HH 212 needs to be confirmed by collecting observations on a statistical sample. Answers are expected soon from the FAUST ALMA Large Program (Fifty AU STudy of the chemistry in the disc/envelope system of Solar-like protostars, http://faust-alma.riken.jp) and from the ALMA-DOT program (ALMA

chemical survey of disc-outflow sources in Taurus, Garufi et al. 2020b). The goal of these projects is to reveal the chemical composition of the envelope/disc system on Solar System scale in a sample of discs from the protostellar to the protoplanetary stages.

In order to test the inheritance scenario, i.e. whether the molecular setup of protoplanetary discs is largely inherited from the molecular clouds from which the stars formed, it is also crucial to compare the chemical composition of protostellar objects with that of Solar System objects (the final stage of Sun-like stars formation process). Comets are ideal for this purpose, as they sample the pristine composition of the outer Solar System. A comparative study of the comet 67P Churyumov-Gerasimenko, visited and characterized in detail by the ESA mission Rosetta, with two Solar-like protostellar systems, IRAS16293-2422B and SVS13-A, shows similar abundances of NH_2CHO and $HCOOCH_3$, and in general of CHO-, N- and S-bearing species, which suggests inheritance from the presolar phase (Bianchi et al., 2019; Drozdovskaya et al., 2019). Also in this case these promising results need to be confirmed by further comparative studies.


6 Giant Planets and their Composition

Giant planets, from Neptune-like to super-Jovian planets, currently represent the bulk of Ariel's observational sample (Edwards et al., 2019): as a result, efforts are being devoted to improve our understanding of what factors can shape their atmospheric composition as will be observed by Ariel (Turrini et al., 2018). In the following we focus on three of these factors: the link between orbital migration and metallicity (Sect. 6.1), the distribution of accreted material between the core and the growing envelope (Sect. 6.2), and the compositional features arising from different migration histories (Sect. 6.3).

6.1 Planetary migration and bulk metallicity

Many hot Jupiters are found to be highly enriched in heavy elements compared to their stellar-host metallicity. Theory suggests that some of these planets are expected to consist of several tens and even hundreds of Earth-masses of heavy elements (although still with large uncertainties, see Miller and Fortney, 2011; Thorngren et al., 2016; Wakeford et al., 2017; Sing, 2018). This introduces great challenges to the giant planet formation theories since the expected enrichment from the standard formation process is very moderate and typically cannot exceed about 20 $M_\oplus$ (e.g. Shibata and Ikoma, 2019). As a result, the enrichment of the planets must be explained.

One could imagine that the planetary enrichment occurs after the planet has formed and gas accretion terminated, a natural pathway being planetesimal capture. This process, however, is quite inefficient once the giant planets approach their final mass values (being able to supply a few Earth-masses
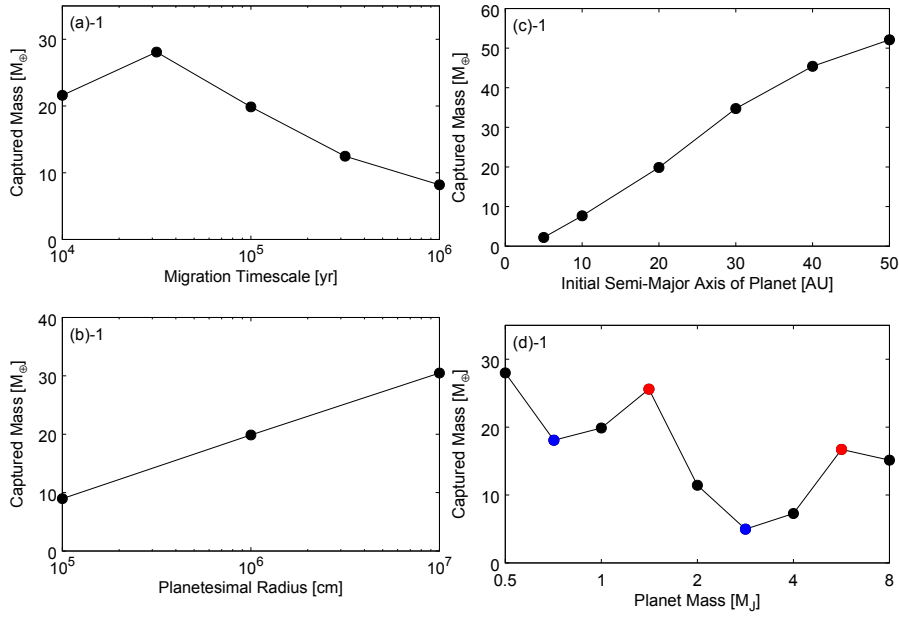
Fig. 4 Results of the parameter study of planetesimal capture by a migrating protoplanet performed by Shibata et al. (2020). Shown is the total mass of captured planetesimals in Earth masses as a function of: the migration timescale of the planet (a)-1, the radius of planetesimals (b)-1, the initial semi-major axis of the planet (c)-1, and the mass of the planet (d)-1.

of heavy elements at most, Turrini et al., 2015, and references therein) and becomes even less efficient in presence of post-formation migration. Shibata et al. (2020) and Turrini et al. (2021) recently investigated the enrichment of warm gas giants via planetesimal capture during inward migration. Shibata et al. (2020) performed orbital simulations of migrating giant planets of different masses and planetesimals in a protoplanetary gaseous disc and inferred the heavy-element mass that is accreted by the planet. Turrini et al. (2021) focused on Jovian planets but traced also their mass and radius evolution during their migration.

Shibata et al. (2020) found that **migrating giant planets capture planetesimals with total masses of several tens of Earth masses**, if the planets start their formation at tens of au in relatively compact discs (less than 100 au, as generally assumed for the solar nebula). A similar result is obtained in the study by Turrini et al. (2021) focusing on large (gas extending to a few 100 au) but not exceedingly massive discs (disc masses of the order of a few 10^{-2} $M_{\odot}$) if the giant planets have formation regions comparable to those recently observed by ALMA, i.e. extending from a few tens to about a hundred au from the host star (e.g. Andrews et al., 2018).

Depending on the characteristics of the considered protoplanetary disc, planetesimal capture seems to be efficient in a rather limited range of semi-major axis (Shibata et al., 2020) or for migration tracks spanning several tens of au (Turrini et al., 2021). Nevertheless, both studies showed that the total captured planetesimal mass increases with increasing migration distances. It was also shown that mean motion resonances trapping and aerodynamic gas drag inhibit planetesimal capture of a migrating planet, and therefore large scale migration and/or massive/enriched discs are required to explain the enrichment of planets with several tens Earth masses of heavy elements.

Figure 4 summarizes the results of the study performed by Shibata et al. (2020), which suggests that enriched giant exoplanets at small orbits have not formed *in situ* since they must have migrated inward in order to accrete large amounts of heavy elements. As will be discussed in more detail in Sect. 8, however, recent population studies investigating the architectures of known multi-planets extrasolar systems (Zinzi and Turrini, 2017; Laskar and Petit, 2017; Turrini et al., 2020; He et al., 2020) suggest that a significant fraction of these planetary systems underwent or are crossing phases of chaotic evolution possibly associated to migration by planet-planet scattering (Rasio and Ford, 1996; Weidenschilling and Marzari, 1996).

A widespread presence of chaos-driven migration in the life of planetary systems, in alternative or in conjuction with disc-driven migration, would introduce a layer of uncertainty in unequivocally linking the formation and dynamical history to its heavy element enrichment. As an example, a giant planet forming and migrating between 30 and 20 au while embedded in the disc, as in the accretion tracks by Shibata et al. (2020), and later being scattered to a fraction of au by planet-planet scattering could be characterized by the same heavy element enrichment than a giant planet that started forming at about 10 au and experienced only disc-driven migration (see e.g. the top right panel of Fig. 4). As we will illustrate in Sect. 6.3, however, the different compositional signatures of the accreted heavy elements allow for breaking this degeneracy.

6.2 Envelope enrichment through core formation

Several recent works follow the ablation of accreted solids in the gaseous envelope in the planet formation phase and find a significant pollution of the growing gas envelope by the accreted solids (e.g. Brouwers et al., 2018; Valletta and Helled, 2018; Bodenheimer et al., 2018). It is found that when the planetary core mass is less than a few Earth masses most of the accreted solids, both rocks and ices, are deposited in the gaseous envelope and don't reach the core. As the formation processes continues, the internal temperatures increase, the gravity becomes stronger and the gas is denser, and thus a larger fraction of the solids stays in the envelope.

> The resulting structure right after the planet formation is then of a **gradual composition distribution instead of a core-envelope structure**. This primordial gradual metal distribution may evolve to a metal enrichment of the envelope in the long term. Under certain conditions, that are common in gas giant interiors, convection and therefore **convective-mixing can spread the composition gradient to the outer envelope in time**, and increase the outer envelope metallicity (Vazan et al., 2015).

The measured metal enrichment by the Ariel mission, and the derived statistics for different planetary types, can be used to constraint the formation outcomes and the convective behaviour. For example, in absence of fragmentation the envelope enrichment is greater in the case of pebble accretion than in planetesimal accretion. As is shown in the left panel of Fig.5, pebbles dissolve better and earlier in the envelope than planetesimals, and therefore results in a more enriched envelope for the same planetary mass. The break-up of planetesimals during accretion can enhance the envelope pollution that is shown in Fig.5 (Mordasini et al., 2015; Valletta and Helled, 2018). Overall, ablation of pebbles is more efficient for small core/envelope masses while planetesimal break-up and ablation play a significant role for envelope masses greater than a few Earth masses (Mordasini et al., 2015; Podolak et al., 2020).

After the formation phase the local metal enrichment can be redistributed in the planet's envelope by convective-mixing. Long-term evolution of the structure by convective-mixing successfully explains the properties of our Solar System giant planets (Vazan et al., 2016, 2018; Vazan and Helled, 2020), and is expected to take place in giant exoplanet interiors. The efficiency of the mixing depends on the metals distribution: an outer moderate enrichment tend to mix efficiently, while a deeper steeper distribution remains stable, as is shown in the right panel of Fig.5 for Jupiter. Thus, the initial metal enrichment by the formation building blocks affects the long-term atmospheric abundances of the planet.
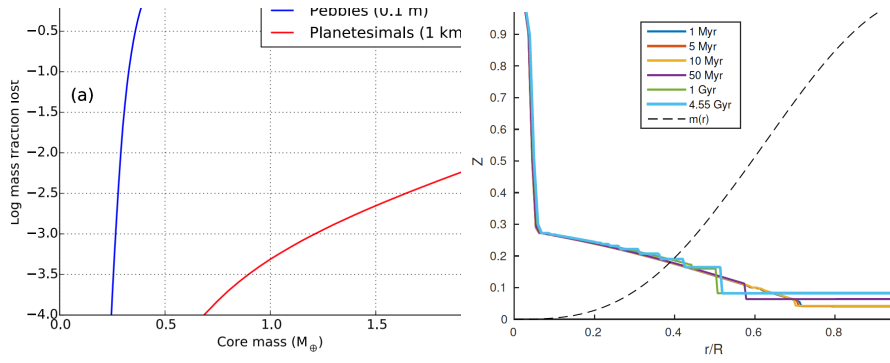
Fig. 5 *Left:* Mass deposition in the envelope (lost) as a function of the growing core mass, for rocky planetesimals (red) and pebbles (blue). Fragmentation is ignored. Rocky planetesimals lose approximately 1% of their mass when the forming planet has a core mass of 2 Earth masses, whereas the pebbles are fully evaporated before the planet's core mass reaches 0.5 Earth mass (Brouwers et al., 2018). *Right:* the change in time in the metal distribution (Z) in the interior of Jupiter. At early ages convective-mixing is efficient in the outer shallow composition gradient, while the inner steeper gradient remains stable Vazan et al. (2018).
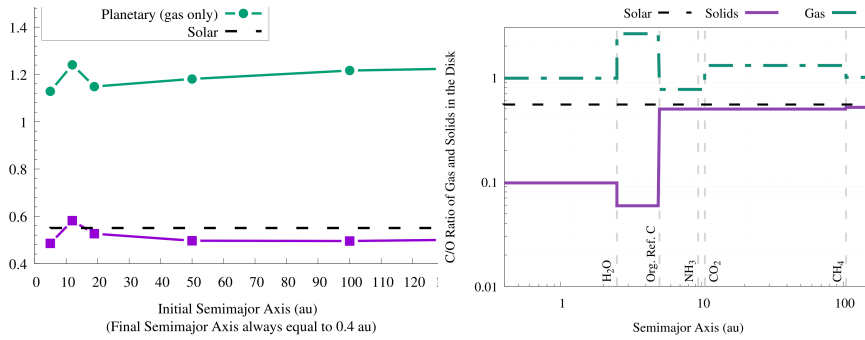
Fig. 6 *Left* : C/O ratio of giant planets undergoing extensive migration from formation regions consistent with those observed with ALMA. *Right* : C/O ratio of the gas and solids in the protoplanetary disk taking into account the roles of refractories and refractory organics as carriers of O and C (see main text and Turrini et al. 2021 for details). The CO_2 snowline is located at about 10 au and the disc gas is dominated, from that point outward, by CO and CH_4 ($C/O \gtrsim 1$). As a result, giant planets forming beyond the CO_2 snow line and accreting limited solids will have $C/O \gtrsim 1$, while giant planets accreting large quantities of solids will have C/O slightly smaller than the stellar value. Figure adapted from Turrini et al. (2021).

6.3 Compositional signatures of different formation regions

A number of studies have been devoted in recent years to link the information supplied by the composition of giant exoplanets to their formation and migration histories. Before discussing the insight they provide, however, it is important to point out that their task is made particularly challenging by our still incomplete understanding of the chemical environment of protoplanetary discs, the birthplace of giant planets. As highlighted by the discussions in Sects. 2 and 5, even if modern observational facilites are providing an unprecedented
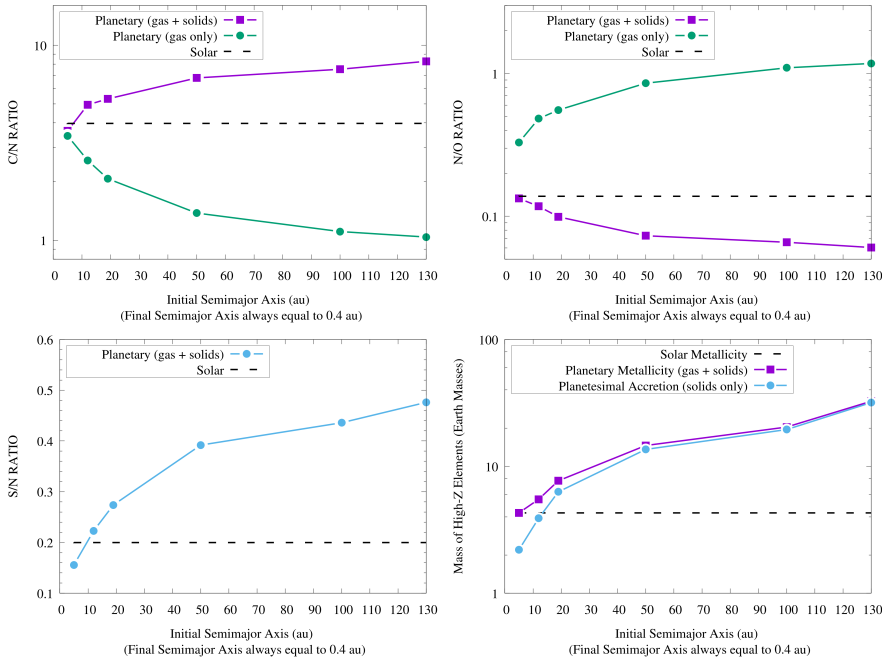
Fig. 7 C/N (top left), N/O (top right) and S/N (bottom left) elemental ratios of a Jupiter-sized giant planet as a function of different formation regions and migration tracks (Turrini et al., 2021). The Jovian planet starts its formation at the specified orbital distances and undergoes disc-driven migration until it becomes an hot Jupiter. The horizontal dashed lines indicate the stellar elemental ratios, assuming a solar composition for the host star and the protoplanetary disc (Palme et al., 2014). The different curves in the top half of the figure refer to different mass growth scenarios involving the accretion of both gas and planetesimals ("gas + solids") or the sole gas ("gas only"). Also shown is the comparison between the total mass of heavy elements accreted by the giant planet and the one due only to planetesimal capture (bottom right), which highlights how the S/N ratio can be used as a proxy into the planetesimal contribution to metallicity. Figure from Turrini et al. (2021).

view of protoplanetary discs, their physical and compositional characterization is still hindered by a number of uncertain parameters and observational limitations. A particularly critical source of uncertainty is associated with the initial molecular setup of protoplanetary discs, as it is unclear whether protoplanetary discs inherit their composition from the prestellar phase or undergo a complete reset due to the radiation environment of their young stars.

As discussed in Sect. 5, the results of the recent comparisons between the volatile inventory of the comets in the Solar System and Solar-like protostellar systems appear to support a strong role of inheritance from the prestellar phase (Drozdovskaya et al., 2019; Bianchi et al., 2019; Altwegg et al., 2019). However, even in this scenario, discs are expected to chemically evolve (Eistrup et al., 2016, 2018) and cool down over time. Their temperature decrease will cause the snowlines of the more volatile elements to drift inward with respect to their original positions (Panić and Min, 2017; Eistrup et al., 2018). Finally,

the differential radial drift of the dust grains with respect to the gas will cause volatile elements initially frozen on the grains to cross the snowlines in the disc and sublimate, locally enriching the gas (Piso et al., 2016; Booth and Ilee, 2019; Bosman et al., 2019). A recent, detailed review of these processes and how they are expected to shape the compositional environment of protoplanetary discs is provided by Oberg and Bergin (2020).

It is important to note, however, that the magnitude of the previously listed effects is linked to the abundance of dust grains and pebbles in discs and that the conversion of dust and pebbles into planetesimals act to reduce the rate of compositional evolution of protoplanetary discs. The smaller surface-to-volume ratio of planetesimals with respect to dust and pebbles will slow down the rate of gas-grain chemistry and, due to the thermal inertia of the planetesimals that effectively isolate the ices trapped in their interior, will limit the effects of ice sublimation at the crossing of snowlines (e.g. Turrini et al., 2021). Observational evidences from both protoplanetary discs (Manara et al., 2018) and meteorites in the Solar System (Scott, 2007) points toward an efficient conversion of the bulk of dust into planetesimals on a timescale of less than 1 Myr, and possibly of the order of 10^5 years (Schiller et al., 2018). Such conversion would thus appear to proceed at a pace comparable or faster than the global evolution timescale (of the order of 1 Myr) estimated by astrochemical models of evolving discs (Eistrup et al., 2018), suggesting the possibility of an early "freezing" of the composition of protoplanetary disks.

While we are still limited by our incomplete understanding of the compositional nature of protoplanetary discs, a growing literature has been focusing over the past decade on exploring the link between the abundances of the two most abundant high-Z elements, carbon (C) and oxygen (O), and the planet formation process (see e.g. Madhusudhan et al., 2016; Madhusudhan, 2019, and references therein for recent overviews). The general expectation since the early results from Öberg et al. (2011) is for low metallicity giant planets, where the bulk of C and O are accreted from the gas, to be characterized by super-solar C/O ratios, while for high-metallicity giant planets, where C and O are dominated by the capture of solids, to be characterized by sub-solar C/O ratios. As a consequence, studies have been investigating the possibility to use the C/O ratio as a proxy into the formation region of giant planets (see e.g. Madhusudhan et al. 2016 and references therein for an overview and Mordasini et al. 2016, Cridland et al. 2019 for recent results).

Critical factors to this end, however, are the distribution of C and O across the different phases (rocks, organics, and ices) and volatile molecules (e.g. H_2O, CO_2, CO, CH_4), our understanding of which has been significantly evolving over the past decade thanks to the data provided by meteorites, comets, polluted white dwarfs, and protoplanetary discs (e.g. Lodders, 2010b,a; Öberg et al., 2011; Johnson et al., 2012; Palme et al., 2014; Thiabaud et al., 2014; Marboeuf et al., 2014b,a; Bergin et al., 2015; Mordasini et al., 2016; Bardyn et al., 2017; Isnard et al., 2019; Doyle et al., 2019; Cridland et al., 2019; Altwegg et al., 2019; Fulle et al., 2019; Rubin et al., 2020; Turrini et al., 2021), and the extension of the planet-forming region in discs, recently put into ques-

tion by observational surveys of protoplanetary discs with ALMA (e.g. ALMA Partnership et al., 2015; Isella et al., 2016; Fedele et al., 2017, 2018; Long et al., 2018; Andrews et al., 2018).

A study performed in the framework of the Ariel Consortium (Turrini et al. 2021, see Fig. 6, left plot) confirms the general picture described above for the planetary C/O ratio also in the case of giant planets forming at tens and beyond one hundred of au from the host star, as suggested by the results of ALMA surveys. The same results, however, show how for giant planets forming so far from their host stars the information provided by the C/O ratio may be less detailed than expected. In the framework of the inheritance scenario coupled with the early conversion of dust into planetesimals considered in the study, the reason for this is easily understood if one considers that, due to their higher volatility, CO and CH_4 condense about a order of magnitude farther aways from the star than CO_2 (see Fig. 6, right plot). This in turn means that over a large fraction of the planet-hosting region suggested by ALMA's observations, the gas in the disc will be populated mainly by CO and CH_4. Giant planets forming beyond the CO_2 snowline will therefore accrete material from a region where the C/O of the gas will be dominated by the contributions of these two molecules (C/O$\gtrsim$1, see the right plot of Fig. 6). While gaseous CO and gaseous CH_4 will increase the C abundance of the gas and reduce that available for condensates, the abundances of these molecules will cause the C/O ratio of solids in this region to be only slightly smaller than the stellar value (see Fig. 6, right plot).

As a result, giant planets starting their formation at orbital distances spanning the range revealed by ALMA surveys will accrete significant fractions of their mass, if not most of it, beyond the CO_2 snowline. Those giant planets whose mass growth is dominated by gas (low metallicity giant planets), e.g. forming across orbital regions previously depleted of planetesimals by the formation and migration of another giant planet, will have C/O$\gtrsim$1 (Turrini et al., 2021). Those capturing significant amounts of solids in the form of planetesimals (high metallicity giant planets) will have C/O slightly below than the stellar value almost independently on their exact formation region (see Fig. 6, left plot, and Turrini et al. 2021). The limited changes in the C/O values shown in the left plot of Fig. 6 are smaller than the accuracy of current retrieval tools (e.g. Barstow et al., 2020), meaning that those C/O values would be observationally indistinguishable from each other. This translates in the fact that the C/O ratio might only allow to distinguish low metallicity, gas-dominated giant planets from high metallicity, solid-enriched giant planets and provide the information that they formed and captured most of their heavy elements farther out than the CO_2 snowline (Turrini et al., 2021).

The picture discussed above has been derived assuming the compositional inheritance of the volatile materials in the protoplanetary disc from the prestellar phase. As discussed at the beginning of this section and in Sect. 5 (see also Altwegg et al. 2019 and Oberg and Bergin 2020 for more detailed discussion), while there are lines of evidence supporting such a scenario, it does not represent the only possible compositional setting for the planet formation

process. The partitioning of the volatile molecules between gas and planetesimals can be markedly different in a compositional reset scenario, in principle making the picture described above for the planetary C/O ratio invalid. As discussed in Turrini et al. (2021), future studies will need to quantify the effects of the different compositional scenarios on the planetary C/O ratio for giant planets forming over a wide range of orbital distances, to clarify the limits of its diagnostic power. Similarly, the effects of different couplings between the planet formation and the disc evolution timescales will need to be explored. Nevertheless, the available observational data on the roles of refractories and refractory organics as carriers of O (Lodders, 2010b,a; Palme et al., 2014; Doyle et al., 2019) and C (Bergin et al., 2015; Bardyn et al., 2017; Isnard et al., 2019) support the possibility that the quantitative changes in the planetary C/O ratio between one compositional scenario and another could be less marked than previously thought and, consequently, that the C/O ratio may provide only limited information.

The vast coverage of Ariel in terms of molecules offers a straightforward way out of this limitation by allowing for the use of multiple elemental ratios (Tinetti et al., 2018; Turrini et al., 2018). An illustrative example is provided by Fig. 7, which shows the results obtained in the study by (Turrini et al., 2021) using an extended set of four elemental ratios including, in addition to C and O, other cosmically abundant elements as nitrogen (N) and sulphur (S). The inclusion of N alongside C and O allows for computing two additional ratios: N/O and C/N. Due to their higher volatility of N with respect to C and O, the N/O ratio grows with migration for low metallicity giant planets and decreases for high metallicity ones, while C/N behaves the opposite way. The farther the giant planet starts its migration from the host star, the more its C/N and N/O ratios will diverge from the stellar ones (Turrini et al., 2021).

The inclusion of S alongside N allows for computing the S/N ratio: given that the bulk of S is efficiently trapped into refractory solids (e.g. Lodders, 2010b,a; Palme et al., 2014; Kama et al., 2019) while the bulk of N remains in gas phase as highly volatile N_2 for most of the extension of discs (e.g. Pollack et al., 1994; Eistrup et al., 2016, 2018; Öberg and Wordsworth, 2019; Bosman et al., 2019), this ratio offers a direct probe into the planetary metallicity and, specifically, the fraction of the planetary metallicity due to the accretion of planetesimals (see Fig. 7). The S/N ratio, therefore, can be used to constrain, independently on the knowledge of the planetary mass and radius, the disc-driven migration experienced by the giant planet as discussed in Sect. 6.1 (see Turrini et al. 2021 for a discussion). Recent works focusing on the study of Jupiter's formation in the Solar System (Öberg and Wordsworth, 2019; Bosman et al., 2019) further highlighted how the combination between a super-stellar metallicity (e.g. obtained through the mass-radius relationship) with a stellar S/N ratio in a giant planet can indicate its formation beyond the N_2 snowline (N_2 being the main N carrier in protoplanetary discs). Note that, due to its high volatility, N_2 condenses as ice at a few tens of au even in cold discs (Eistrup et al., 2016, 2018; Öberg and Wordsworth, 2019), while for warmer discs (e.g. 280 K at 1 au, as generally assumed for the solar nebula and adopted

by Turrini et al. 2021) N_2 may remain in gas form until a few hundreds of au from the star, farther out than even the planet-hosting region suggested by ALMA's surveys.

> The use of **multiple elemental ratios involving elements of different volatility** permitted by Ariel's spectral coverage allows to greatly **reduce the degeneracy intrinsic in any single measure** and to more robustly constrain the formation and dynamical history of giant planets (Turrini et al., 2021).

It is important to point out that the discussion above focuses on specific absolute values that have been derived assuming a composition of the proto-planetary disc matching the protosolar composition (see e.g. Asplund et al., 2009; Lodders, 2019, and references therein). As discussed in Sect. 4, different stars will be characterized by different metallicities and, more importantly, different elemental ratios. As a result, the elemental ratios of planets orbiting different stars cannot be directly compared and the specific values reported above (e.g. C/O > 1) should not be considered as absolute references.

This obstacle can be overcome with the use of planetary elemental ratios normalised to their relevant stellar values, analogously to the case of the normalized metallicities values adopted by Thorngren et al. (2016). The use of normalized elemental ratios (not necessarily limited to the cases of C/N, N/O, C/O and S/N discussed above) removes the intrinsic compositional variability between different planetary systems and opens up the possibility of more reliable comparisons between the respective formation and migration histories of giant planets orbiting different stars.

Furthermore, as discussed by Turrini et al. (2021) the use of normalized elemental ratios associated with elements characterized by different volatility provides additional constraint on the nature of giant planets. The C/O, C/N, N/O and S/N ratios normalised to their stellar values (indicated with the superscript *) reveal that high metallicity giant planets will be characterized by C/N* > C/O* > N/O* (see Fig. 8). Gas-dominated, low metallicity giant planets, instead, will be characterized by N/O* > C/O* > C/N* (see Fig. 8). Giant planets for which planetesimal accretion is the main source of metallicity will have S/N* > C/N*, while those for which both gas and solids contribute to the metallicity will have instead C/N* > S/N* (see Fig. 8).

Finally, since the normalization to the stellar values brings the planetary elemental ratios of elements with different cosmic abundances on a common scale, any element whose main carrier is characterized by a lower or similar volatility than S (see e.g. Palme et al., 2014; Turrini et al., 2018) can be used to compute normalized elemental ratios with respect to N and gain insight on the source of the planetary metallicity (Turrini et al., 2021). The use of normalized elemental ratios therefore allows to compare the constraint on the metallicity derived for different giant planets using different low-volatility elements (e.g. S/N*,Al/N*,Na/N*,Cr/N*).
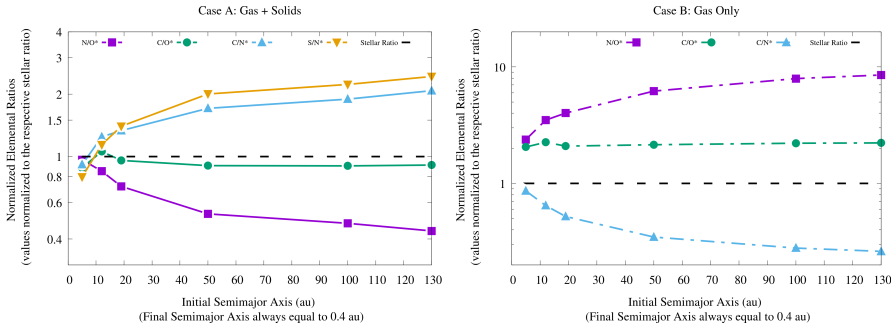
Fig. 8 *Left:* comparison of the normalized C/O, N/O, C/N, and S/N elemental ratios of the gaseous envelope when the metallicity of the giant planet is dominated by the accretion of planetesimals (high metallicity case). *Right:* comparison of the normalized elemental ratios in the gaseous envelope when the metallicity of the giant planet is dominated instead by the accretion of gas (low metallicity case). Each elemental ratio is normalized to the relevant stellar elemental ratio. Figure from Turrini et al. (2021).

7 High-density Planets: Formation and Atmospheres

The *Kepler* exoplanet survey revealed that a vast majority of close-in exoplanets are smaller in size than Neptune (Batalha, 2014). Such planets are called *high-density planets* in this manuscript, as the bulk of their mass is represented by condensates with higher densities that the gas providing most of the mass of gas giants like Jupiter and Saturn. Given their high occurrence, understanding their formation is a central issue in exoplanetary science.

High-density planets, in general, are formed in a complicated way through various processes including solid and gas accretion, orbital migration, giant collisions, late veneers, mass loss, etc. Thus, the sole knowledge of basic physical properties such as mass, radius, and orbital elements is not enough to unveil their nature (e.g. Tinetti et al., 2018; Turrini et al., 2018, and references therein). The characterisation of their bulk and atmospheric compositions is therefore the key to understand the formation and diversity of low-gravity planets (Tinetti et al., 2018; Turrini et al., 2018).

One of the biggest uncertainties in the planet formation process is the orbital migration that occurs via angular momentum exchange between the planet and the circumstellar disc (the so-called type-I migration). Planetary migration leads to the delivery of cold materials from beyond the snowline to the inner regions of discs and, thus, brings about a variety in composition of close-in planets. Since planetary migration occurs in a circumstellar disc composed predominantly of hydrogen and helium, migrating planets generally capture the surrounding disc gas by gravity to form an atmosphere. Such atmospheres of high-density planets are often termed primordial atmospheres or captured atmospheres.

Figure 9 shows the predicted masses, radii, and volatile contents of synthesised planets around M dwarfs of 0.3 $M_\odot$ with slow (*left panel*) and fast
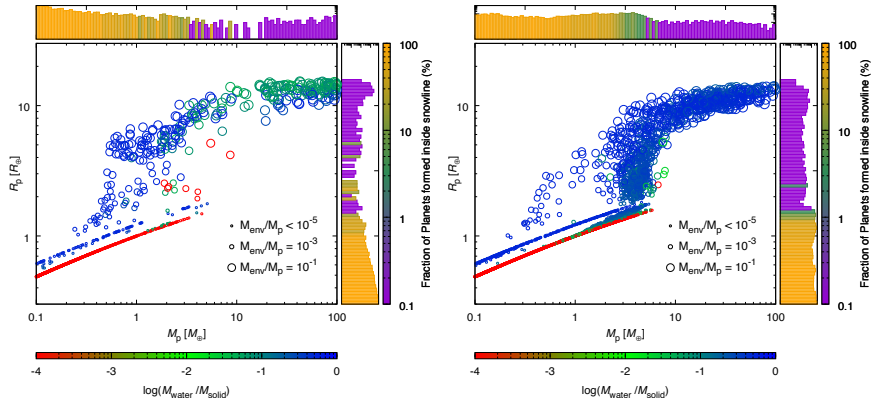
Fig. 9 Theoretical prediction of masses, radii, and volatile contents of planets around a $0.3\ M_\odot$ star. The population synthesis models include planetesimal accretion, gas accretion, orbital migration, collision of planetary embryos, viscous dissipation of the protoplanetary disc, and photo-evaporation of planetary atmospheres (Miguel et al., 2019, Kimura et al. in prep.). The rate of the type-I migration differs between the two panels: In the left and right panels, 1% (slow) and 10% (fast), respectively, of the migration rate from Tanaka et al. (2002) are assumed. The synthesised planets are composed of a solid body (ice plus rock) and a H-He atmosphere. In the mass-radius relationship diagram, symbols are colour-coded according to the total mass of water, which comes from icy planetesimals, and are sized according to the atmospheric mass relative to the solid planet mass. Also, in the mass and radius histograms, where the number is given in log, the colour coding indicates the percentage of planets formed inside the snowline. The synthesised planets have been sampled according to their transit probabilities.

(*right panel*) migration. Here we have carried out those calculations by adding the effects of atmospheric accumulation and loss (Kimura and Ikoma, 2020) in the population synthesis models (Miguel et al., 2019). The symbols for radii of 1–4 $R_\oplus$ are shown with different colours and sizes, indicating that the high-density planets are diverse in bulk composition; namely, they have different ice-to-rock ratios and different atmospheric masses. As seen in the histograms, the bulk composition of high-density planets also differs depending on the migration rate. Thus, knowledge of bulk composition places a crucial constraint to migration rates. It is noticed, however, that some of the planets in Figure 9 have the same mass-radius relationships but different composition. Such degeneracy in composition prevents us from constraining the bulk composition (see also Turrini et al., 2018, for a discussion). Observation of their atmospheres with Ariel is of obvious significance.

While the disc gas consists predominantly of hydrogen, the atmospheres are not always hydrogen-dominated. Instead, they would contain heavier molecules than H_2 and He. Such contamination (or enrichment) occurs because of degassing from volatile-rich planetesimals and magma oceans (e.g. Nikolaou et al., 2019) and chemical interaction between the atmospheric gas and minerals from magma oceans (e.g. Kimura and Ikoma, 2020). In some extreme cases, the planets might lose all their primary atmosphere due to evaporation

processes and interaction with the host star, and might have an outgassed, secondary atmosphere (Miguel et al., 2011; Nikolaou et al., 2019).

A mixture of both acquired and core-degassed volatiles is likely to form the atmospheric inventory. Moreover, the specifics of how volatile species chemically bond with rocky interiors found in solid (silicate mantle) or molten (magma ocean) state suggest that the sources of less soluble versus soluble species may differ. That is, CO and CO_2 that are less soluble in silicate melts could be provided directly from the captured disc gas, while H_2O could be provided from thermal evolution of the interior (Nikolaou et al., 2019) as well as upper atmosphere chemistry (Ikoma and Genda, 2006). Thus, detailed investigation of atmospheric constituents helps us understand such processes, including contamination by and partitioning processes of heavy volatiles.

Contamination of heavy elements, however, tends to reduce the atmospheric scale height due to increase in mean molecular weight (μ), and thereby hinders atmospheric characterisation via transmission spectroscopy. Figure 10 shows the relationship between the total mass of H_2O contained in the atmosphere and the mean molecular weight of the atmospheric gas for several choices of the solid planet mass by the same method as Kimura and Ikoma (2020). Here we have calculated the structure and mass of the atmosphere enriched with water that is connected to the circumstellar gas disc. For reference, the orange symbols indicate the maximum amounts of volatiles that can be degassed from a magma ocean with H_2O content of 1 %.

As shown in this figure, the mean molecular weight of the atmosphere is at most five, which is about twice as high as that of the atmospheric gas with solar abundances. Note that we have ignored any carbon-based molecules such as CO_2 here for simplicity; for the gas of $\mu = 5$, for example, if H_2O is replaced completely with CO_2, μ increases (and, thus, the pressure scale height decreases) by 10 %.

> Ariel has the capability to **constrain the atmospheric mean molecular weight of high density planets** (Edwards et al., 2019). This can be achieved already with Tier 1 resolution for the most favourable cases. In the less favourable cases, additional observational time will be required to constrain the mean molecular weight, though this additional time is estimated to be less than what would be needed to achieve full Tier 2 resolution (Edwards et al., 2019).

More refined assessments are ongoing (Mugnai et al., in preparation), with a particular focus on verifying the possibility of coupling the estimation of the atmospheric mean molecular weight with the detection of the main molecular constituents (especially water, Turrini et al. 2018). Nevertheless, the current picture indicates that Ariel should be able to provide indications on the *primary/secondary atmospheres ratio among high-density planets* (Turrini et al., 2018; Edwards et al., 2019).
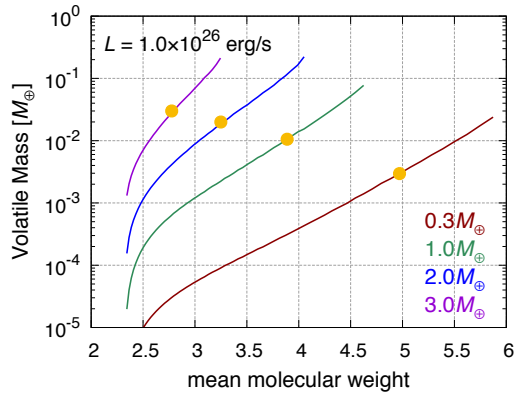
Fig. 10 Possible range of mean molecular weight of the atmospheric gas for sub- and super-Earths. We have calculated the mass of the enriched atmosphere in dynamical equilibrium with the protoplanetary disc as a function of the mean molecular weight by the same method as Ikoma et al. (2018) and Kimura and Ikoma (2020). The orange symbols indicate the maximum amounts of volatile that would be degassed from a magma ocean with water content of 1 %. In these calculations we have assumed that the planet is located at 0.2 AU from an M dwarf of 0.3 $M_\odot$ and the energy flux in the atmosphere is 1×10^{26} erg/s.

8 Planetary Architectures: Dynamical Context to Composition

Before moving to the conclusions it is worth emphasizing once again that, as discussed in Sect. 6.1, disc-driven migration is not the only dynamical process capable of delivering giant planets from their formation regions to the orbital distances where Ariel will observe them today. Other migration mechanims (planet-planet scattering, ejection from resonances, orbital chaos) can achieve the same outcome while having markedly different implications for the composition of the planets they affect (see e.g. Turrini et al., 2015, 2018, and references therein). Furthermore, as discussed in Sect. 3 there is emerging evidence suggesting a role played by the galactic environment in shaping the characteristics of planetary systems.

Recent population studies of multi-planet systems highlight how their architectures record a strong role of violent processes, such as chaos and planet-planet scattering, in shaping the dynamical histories of known exoplanets (Limbach and Turner, 2015; Zinzi and Turrini, 2017; Laskar and Petit, 2017; Turrini et al., 2020; He et al., 2020; Bach-Møller and Jørgensen, 2021). As such mechanisms act when most solid mass in planetary systems has been incorporated into a limited number of massive bodies, the migrating planets they produce will encounter and accrete less material than their counterparts migrating in protoplanetary discs. At the same time, however, stochastic encounters between planets may result in catastrophic collisions with major

implications for the composition and interior structure of the emerging planet.

> Consequently, this strong **role played by migration mechanisms other than disc-driven migration introduces a layer of uncertainty** in linking Ariel's compositional data to the formation histories of the observed exoplanets. The same population studies, however, suggest that the combined use of **metrics linked to the angular momentum of planetary systems** (Zinzi and Turrini, 2017; Laskar and Petit, 2017; Turrini et al., 2020) allows for extracting information from their architectures and **constrain their dynamical past**.

In particular, Turrini et al. (2020) and Carleo et al. (2021) have shown how the information provided by the normalized angular momentum deficit (NAMD), an architecture-agnostic measure of the dynamical excitation of planetary systems, allows to build a relative scale of violence of their past histories. Intuitively, the NAMD can be interpreted as the "dynamical temperature" of planetary systems: the higher the value, the more excited is the dynamical state of the system. As in the case of temperature, if one can identity meaningful reference values (as with the freezing and boiling points of water), it is possible to build a scale of dynamical excitation on which to measure the violence of the past of planetary systems.

As discussed by Turrini et al. (2020) and Carleo et al. (2021), Trappist-1 and the Solar System provide two such reference values, the first as a system characterized by an orderly and stable evolution (Tamayo et al., 2017; Papaloizou et al., 2018) while the second as the boundary between orderly and chaotic evolution (Nesvorný, 2018). As shown in Fig. 11 the higher the NAMD of a planetary system with respect to that of the Solar System, the higher the likeliness that chaos and violent dynamical events sculpted its past. Conversely, NAMD values increasingly closer to that of Trappist-1 are associated to increasing likeliness of stable and orderly histories.

As a consequence, the measure of the "dynamical temperature" of planetary systems permitted by the NAMD can provide a dynamical context for the interpretation of Ariel's compositional observations. In other words, the *combination of Ariel's observations* with the information provided by *planetary system architecture* (specifically masses and orbital elements of its planets) will allow to extract additional and more detailed information on the history of the planets and their host system. It should be noted that the planetary physical and dynamical parameters don't need to be known at the time of Ariel's observations but can be included in the interpretation of Ariel's data at a later time, meaning that *Ariel's scientific impact will grow over time*
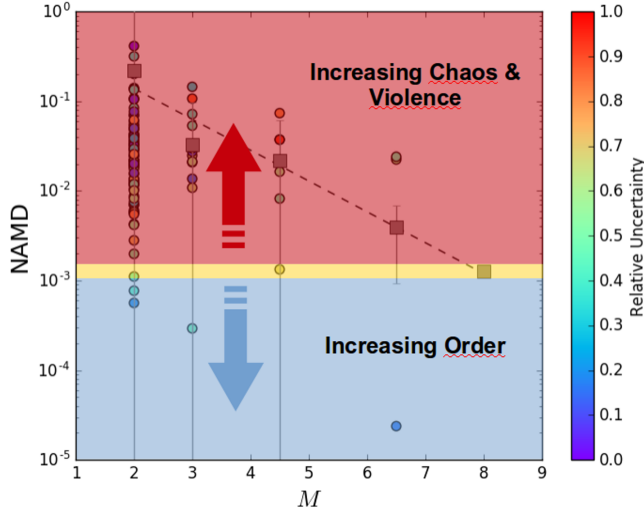
Fig. 11 Illustrative example of "dynamical temperature" scale built using Trappist-1 and the Solar System as reference systems. The underlying plot shows the dynamical excitation, quantified by the NAMD, of the 99 best-characterized planetary systems (filled circles) grouped according to the multiplicity of the planetary systems (i.e. their number of planets) with the systems with $M=4$ and $M=5$ and with $M=6$ and $M=7$ respectively grouped together to increase the statistics. Each planetary system is color-coded according to the relative uncertainty of its NAMD value. Also shown are the mean NAMD values of each multiplicity population (filled squares), computed as weighted-averages over the uncertainties of the individual systems. The overlaid coloured areas showcase an illustrative division between increasing likelyness of dynamical violence (red) and orderly evolution (blue), separated by an uncertainty region (yellow) centered on the Solar System. Figure adapted from Turrini et al. (2020).

9 Concluding Remarks

As introduced in Sect. 1 and further discussed in Sects. 6, 7, and 8, the planet formation process plays a fundamental role in shaping the final composition of planets and, consequently, of their atmospheres. Ariel's observations will therefore provide an unprecedented wealth of data to advance our understanding of planet formation in our Galaxy. However, as the discussion in Sects. 2-5 highlights, a number of *environmental factors* linked to the star and its own formation process *affect the final outcome*: the galactic environment in which the star formation process takes places, the stellar composition and the thermal and physical structure and evolution of the protoplanetary disc.

As the implications of these environmental factors are still poorly constrained or understood, they can act as a *source of uncertainty* or noise in the interpretation of the atmospheric data Ariel will provide and the reconstruction of the formation and evolution history of the observed planets. As a consequence, care should be taken, particularly during the initial phases of the

nominal mission, to *keep these factors into account in the selection of Ariel's targets* (and their stellar hosts) to *minimize the free parameters* in this already complex problem.

The same considerations expressed above, however, also mean that the *potential impact of Ariel's observations for understanding and quantifying the role played by these environmental factors is huge*, particularly when considering an extended mission and the even larger and more diverse observational sample it will bring. As illustrated in particular in Sect. 6, the wide spectral coverage and the resulting large number of molecules that can be traced by Ariel means that the mission is uniquely suited to explore in unprecedented details and from different angles the *link between the star formation and the planet formation processes*.

Acknowledgments

References

Adamo A, Kruijssen JMD, Bastian N, Silva-Villa E, Ryon J (2015) Probing the role of the galactic environment in the formation of stellar clusters, using M83 as a test bench. MNRAS452(1):246–260, DOI 10.1093/\mnras/stv1203, 1505.07475

Adamów M, Niedzielski A, Villaver E, Nowak G, Wolszczan A (2012) BD+48 740—Li Overabundant Giant Star with a Planet: A Case of Recent Engulfment? ApJ754(1):L15, DOI 10.1088/2041-8205/754/1/L15, 1206.4938

Adamów M, Niedzielski A, Villaver E, Wolszczan A, Nowak G (2014) The Penn State - Toruń Centre for Astronomy Planet Search stars. II. Lithium abundance analysis of the red giant clump sample. A&A569:A55, DOI 10.1051/0004-6361/201423400, 1407.4956

Adams FC (2010) The Birth Environment of the Solar System. ARA&A48:47–85, DOI 10.1146/annurev-astro-081309-130830, 1001.5444

Adibekyan VZ, Santos NC, Sousa SG, Israelian G, Delgado Mena E, González Hernández JI, Mayor M, Lovis C, Udry S (2012) Overabundance of α-elements in exoplanet-hosting stars. A&A543:A89, DOI 10.1051/0004-6361/201219564, 1205.6670

Adibekyan VZ, Figueira P, Santos NC, Mortier A, Mordasini C, Delgado Mena E, Sousa SG, Correia ACM, Israelian G, Oshagh M (2013) Orbital and physical properties of planets and their hosts: new insights on planet formation and evolution. A&A560:A51, DOI 10.1051/0004-6361/201322551, 1311.2417

Adibekyan VZ, González Hernández JI, Delgado Mena E, Sousa SG, Santos NC, Israelian G, Figueira P, Bertran de Lis S (2014) On the origin of stars with and without planets. T_c trends and clues to Galactic evolution. A&A564:L15, DOI 10.1051/0004-6361/201423435, 1404.4514

Agúndez M, Roueff E, Le Petit F, Le Bourlot J (2018) The chemistry of disks around T Tauri and Herbig Ae/Be stars. A&A616:A19, DOI 10.1051/0004-6361/201732518, 1803.09450

Aikawa Y, Herbst E (1999) Molecular evolution in protoplanetary disks. Two-dimensional distributions and column densities of gaseous molecules. A&A351:233–246

Alibert Y, Mordasini C, Benz W (2004) Migration and giant planet formation. A&A417:L25–L28, DOI 10.1051/0004-6361:20040053, astro-ph/0403574

Alibert Y, Mordasini C, Benz W (2011) Extrasolar planet population synthesis. III. Formation of planets around stars of different masses. A&A526:A63, DOI 10.1051/0004-6361/201014760, 1101.0513

ALMA Partnership, Brogan CL, Pérez LM, Hunter TR, Dent WRF, Hales AS, Hills RE, Corder S, Fomalont EB, Vlahakis C, Asaki Y, Barkats D, Hirota A, Hodge JA, Impellizzeri CMV, Kneissl R, Liuzzo E, Lucas R, Marcelino N, Matsushita S, Nakanishi K, Phillips N, Richards AMS, Toledo I, Aladro R, Broguiere D, Cortes JR, Cortes PC, Espada D, Galarza F, Garcia-Appadoo D, Guzman-Ramirez L, Humphreys EM, Jung T, Kameno S, Laing RA, Leon S, Marconi G, Mignano A, Nikolic B, Nyman LA, Radiszcz M, Remijan A, Rodón JA, Sawada T, Takahashi S, Tilanus RPJ, Vila Vilaro B, Watson LC, Wiklind T, Akiyama E, Chapillon E, de Gregorio-Monsalvo I, Di Francesco J, Gueth F, Kawamura A, Lee CF, Nguyen Luong Q, Mangum J, Pietu V, Sanhueza P, Saigo K, Takakuwa S, Ubach C, van Kempen T, Wootten A, Castro-Carrizo A, Francke H, Gallardo J, Garcia J, Gonzalez S, Hill T, Kaminski T, Kurono Y, Liu HY, Lopez C, Morales F, Plarre K, Schieven G, Testi L, Videla L, Villard E, Andreani P, Hibbard JE, Tatematsu K (2015) The 2014 ALMA Long Baseline Campaign: First Results from High Angular Resolution Observations toward the HL Tau Region. ApJ808(1):L3, DOI 10.1088/2041-8205/808/1/L3, 1503.02649

Altwegg K, Balsiger H, Fuselier SA (2019) Cometary Chemistry and the Origin of Icy Solar System Bodies: The View After Rosetta. ARA&A57:113–155, DOI 10.1146/annurev-astro-091918-104409, 1908.04046

Andrews SM, Huang J, Pérez LM, Isella A, Dullemond CP, Kurtovic NT, Guzmán VV, Carpenter JM, Wilner DJ, Zhang S, Zhu Z, Birnstiel T, Bai XN, Benisty M, Hughes AM, Öberg KI, Ricci L (2018) The Disk Substructures at High Angular Resolution Project (DSHARP). I. Motivation, Sample, Calibration, and Overview. ApJ869(2):L41, DOI 10.3847/2041-8213/aaf741, 1812.04040

Ansdell M, Williams JP, van der Marel N, Carpenter JM, Guidi G, Hogerheijde M, Mathews GS, Manara CF, Miotello A, Natta A, Oliveira I, Tazzari M, Testi L, van Dishoeck EF, van Terwisga SE (2016) ALMA Survey of Lupus Protoplanetary Disks. I. Dust and Gas Masses. ApJ828(1):46, DOI 10.3847/0004-637X/828/1/46, 1604.05719

Ansdell M, Williams JP, Manara CF, Miotello A, Facchini S, van der Marel N, Testi L, van Dishoeck EF (2017) An ALMA Survey of Protoplanetary Disks in the σ Orionis Cluster. AJ153(5):240, DOI 10.3847/1538-3881/aa69c0, 1703.08546

Ardila DR, Herczeg GJ, Gregory SG, Ingleby L, France K, Brown A, Edwards S, Johns-Krull C, Linsky JL, Yang H, Valenti JA, Abgrall H, Alexander RD, Bergin E, Bethell T, Brown JM, Calvet N, Espaillat C, Hillenbrand LA, Hussain G, Roueff E, Schindhelm ER, Walter FM (2013) Hot Gas Lines in T Tauri Stars. ApJS207(1):1, DOI 10.1088/0067-0049/207/1/1, 1304.3746

Armitage PJ (2009) Astrophysics of Planet Formation. Cambridge University Press, DOI 10.1017/CBO9780511802225

Arriagada P (2011) Chromospheric Activity of Southern Stars from the Magellan Planet Search Program. ApJ734(1):70, DOI 10.1088/0004-637X/734/1/70, 1104.3186

Asplund M, Grevesse N, Sauval AJ, Scott P (2009) The Chemical Composition of the Sun. ARA&A47(1):481–522, DOI 10.1146/annurev.astro.46.060407. 145222, 0909.0948

Avenhaus H, Quanz SP, Garufi A, Perez S, Casassus S, Pinte C, Bertrang GHM, Caceres C, Benisty M, Dominik C (2018) Disks around T Tauri Stars with SPHERE (DARTTS-S). I. SPHERE/IRDIS Polarimetric Imaging of Eight Prominent T Tauri Disks. ApJ863(1):44, DOI 10.3847/1538-4357/aab846, 1803.10882

Bach-Møller N, Jørgensen UG (2021) Orbital eccentricity-multiplicity correlation for planetary systems and comparison to the Solar system. MNRAS500(1):1313–1322, DOI 10.1093/mnras/staa3321, 2010.10371

Balog Z, Rieke GH, Su KYL, Muzerolle J, Young ET (2006) Spitzer MIPS 24 μm Detection of Photoevaporating Protoplanetary Disks. ApJ650(1):L83–L86, DOI 10.1086/508707, astro-ph/0608630

Bardyn A, Baklouti D, Cottin H, Fray N, Briois C, Paquette J, Stenzel O, Engrand C, Fischer H, Hornung K, Isnard R, Langevin Y, Lehto H, Le Roy L, Ligier N, Merouane S, Modica P, Orthous-Daunay FR, Rynö J, Schulz R, Silén J, Thirkell L, Varmuza K, Zaprudin B, Kissel J, Hilchenbach M (2017) Carbon-rich dust in comet 67P/Churyumov-Gerasimenko measured by COSIMA/Rosetta. MNRAS469:S712–S722, DOI 10.1093/mnras/stx2640

Barstow JK, Changeat Q, Garland R, Line MR, Rocchetto M, Waldmann IP (2020) A comparison of exoplanet spectroscopic retrieval tools. MNRAS493(4):4884–4909, DOI 10.1093/mnras/staa548, 2002.01063

Bashi D, Helled R, Zucker S, Mordasini C (2017) Two empirical regimes of the planetary mass-radius relation. A&A604:A83, DOI 10.1051/0004-6361/201629922, 1701.07654

Batalha NM (2014) Exploring exoplanet populations with NASA's Kepler Mission. PNAS 111(35):12647–12654, DOI 10.1073/pnas.1304196111, 1409.1904

Bergin EA, Cleeves LI, Crockett NR, Favre C, Neill JL (2013) Chemistry in Star Forming Regions - Herschel Looking Towards ALMA. In: Kawabe R, Kuno N, Yamamoto S (eds) New Trends in Radio Astronomy in the ALMA Era: The 30th Anniversary of Nobeyama Radio Observatory, Astronomical Society of the Pacific Conference Series, vol 476, Astronomical Society of the Pacific, San Francisco, p 185

Bergin EA, Blake GA, Ciesla F, Hirschmann MM, Li J (2015) Tracing the ingredients for a habitable earth from interstellar space through planet formation. Proceedings of the National Academy of Science 112(29):8965–8970, DOI 10.1073/pnas.1500954112, 1507.04756

Bergner JB, Guzmán VG, Öberg KI, Loomis RA, Pegues J (2018) A Survey of CH_3CN and HC_3N in Protoplanetary Disks. ApJ857(1):69, DOI 10.3847/1538-4357/aab664, 1803.04986

Bhandare A, Breslau A, Pfalzner S (2016) Effects of inclined star-disk encounter on protoplanetary disk size. A&A594:A53, DOI 10.1051/0004-6361/201628086, 1608.03239

Bianchi E, Codella C, Ceccarelli C, Vazart F, Bachiller R, Balucani N, Bouvier M, De Simone M, Enrique-Romero J, Kahane C, Lefloch B, López-Sepulcre A, Ospina-Zamudio J, Podio L, Taquet V (2019) The census of interstellar complex organic molecules in the Class I hot corino of SVS13-A. MNRAS483(2):1850–1861, DOI 10.1093/\mnras/sty2915, 1810.11411

Bodaghee A, Santos NC, Israelian G, Mayor M (2003) Chemical abundances of planet-host stars. Results for alpha and Fe-group elements. A&A404:715–727, DOI 10.1051/0004-6361:20030543, astro-ph/0304360

Bodenheimer P, Stevenson DJ, Lissauer JJ, D'Angelo G (2018) New Formation Models for the Kepler-36 System. ApJ868(2):138, DOI 10.3847/1538-4357/aae928, 1810.07160

Bohlin RC, Savage BD, Drake JF (1978) A survey of interstellar H I from Lalpha absorption measurements. II. ApJ224:132–142, DOI 10.1086/156357

Bond JC, O'Brien DP, Lauretta DS (2010) The Compositional Diversity of Extrasolar Terrestrial Planets. I. In Situ Simulations. ApJ715(2):1050–1070, DOI 10.1088/0004-637X/715/2/1050, 1004.0971

Booth AS, Ilee JD (2020) ^{13}C^{17}O suggests gravitational instability in the HL Tau disc. MNRAS493(1):L108–L113, DOI 10.1093/mnrasl/slaa014, 2001.07550

Booth AS, Walsh C, Ilee JD, Notsu S, Qi C, Nomura H, Akiyama E (2019) The First Detection of ^{13}C^{17}O in a Protoplanetary Disk: A Robust Tracer of Disk Gas Mass. ApJ882(2):L31, DOI 10.3847/2041-8213/ab3645, 1908.05045

Booth RA, Ilee JD (2019) Planet-forming material in a protoplanetary disc: the interplay between chemical evolution and pebble drift. MNRAS487(3):3998–4011, DOI 10.1093/mnras/stz1488, 1905.12639

Booth RA, Clarke CJ, Madhusudhan N, Ilee JD (2017) Chemical enrichment of giant planets and discs due to pebble drift. MNRAS469(4):3994–4011, DOI 10.1093/\mnras/stx1103, 1705.03305

Bosman AD, Cridland AJ, Miguel Y (2019) Jupiter formed as a pebble pile around the N$_2$ ice line. A&A632:L11, DOI 10.1051/0004-6361/201936827, 1911.11154

Brittain SD, Najita JR, Carr JS (2009) Tracing the Inner Edge of the Disk Around HD 100546 with Rovibrational CO Emission Lines. ApJ702(1):85–99, DOI 10.1088/0004-637X/702/1/85, 0907.0047

Brouwers MG, Vazan A, Ormel CW (2018) How cores grow by pebble accretion. I. Direct core growth. A&A611:A65, DOI 10.1051/0004-6361/201731824, 1708.05392

Brown JM, Pontoppidan KM, van Dishoeck EF, Herczeg GJ, Blake GA, Smette A (2013) VLT-CRIRES Survey of Rovibrational CO Emission from Protoplanetary Disks. ApJ770(2):94, DOI 10.1088/0004-637X/770/2/94, 1304.4961

Bruderer S, van Dishoeck EF, Doty SD, Herczeg GJ (2012) The warm gas atmosphere of the HD 100546 disk seen by Herschel. Evidence of a gas-rich, carbon-poor atmosphere? A&A541:A91, DOI 10.1051/0004-6361/201118218, 1201.4860

Buchhave LA, Bizzarro M, Latham DW, Sasselov D, Cochran WD, Endl M, Isaacson H, Juncher D, Marcy GW (2014) Three regimes of extrasolar planet radius inferred from host star metallicities. Nature509(7502):593–595, DOI 10.1038/nature13254, 1405.7695

Canto Martins BL, Das Chagas ML, Alves S, Leão IC, de Souza Neto LP, de Medeiros JR (2011) Chromospheric activity of stars with planets. A&A530:A73, DOI 10.1051/0004-6361/201015314, 1103.5332

Carleo I, Desidera S, Nardiello D, Malavolta L, Lanza AF, Livingston J, Locci D, Marzari F, Messina S, Turrini D, Baratella M, Borsa F, D'Orazi V, Nascimbeni V, Pinamonti M, Rainer M, Alei E, Bignamini A, Gratton R, Micela G, Montalto M, Sozzetti A, Squicciarini V, Affer L, Benatti S, Biazzo K, Bonomo AS, Claudi R, Cosentino R, Covino E, Damasso M, Esposito M, Fiorenzano A, Frustagli G, Giacobbe P, Harutyunyan A, Leto G, Magazzù A, Maggio A, Mainella G, Maldonado J, Mallonn M, Mancini L, Molinari E, Molinaro M, Pagano I, Pedani M, Piotto G, Poretti E, Redfield S, Scandariato G (2021) The GAPS Programme at TNG. XXVIII. A pair of hot-Neptunes orbiting the young star TOI-942. A&A645:A71, DOI 10.1051/0004-6361/202039042, 2011.13795

Carney MT, Hogerheijde MR, Loomis RA, Salinas VN, Öberg KI, Qi C, Wilner DJ (2017) Increased H_2CO production in the outer disk around HD 163296. A&A605:A21, DOI 10.1051/0004-6361/201629342, 1705.10188

Carney MT, Hogerheijde MR, Guzmán VV, Walsh C, Öberg KI, Fayolle EC, Cleeves LI, Carpenter JM, Qi C (2019) Upper limits on CH_3OH in the HD 163296 protoplanetary disk. Evidence for a low gas-phase CH_3OH-to-H_2CO ratio. A&A623:A124, DOI 10.1051/0004-6361/201834353, 1901.02689

Carr JS, Najita JR (2008) Organic Molecules and Water in the Planet Formation Region of Young Circumstellar Disks. Science 319(5869):1504, DOI 10.1126/science.1153807

Chevance M, Kruijssen JMD, Longmore SN (2021) When the Peas Jump out of the Pod: How Stellar Clustering Affects the Observed Correlation of Planet Properties in Multi-Planet Systems. ApJ submitted

Ciaravella A, Jiménez-Escobar A, Cecchi-Pestellini C, Huang CH, Sie NE, Muñoz Caro GM, Chen YJ (2019) Synthesis of Complex Organic Molecules in Soft X-Ray Irradiated Ices. ApJ879(1):21, DOI 10.3847/1538-4357/ab211c, 1905.07958

Ciesla FJ, Sandford SA (2012) Organic Synthesis via Irradiation and Warming of Ice Grains in the Solar Nebula. Science 336(6080):452, DOI 10.1126/science.1217291

Cleeves LI, Öberg KI, Wilner DJ, Huang J, Loomis RA, Andrews SM, Guzman VV (2018) Constraining Gas-phase Carbon, Oxygen, and Nitrogen in the IM Lup Protoplanetary Disk. ApJ865(2):155, DOI 10.3847/1538-4357/aade96, 1808.10682

Codella C, Bianchi E, Tabone B, Lee CF, Cabrit S, Ceccarelli C, Podio L, Bacciotti F, Bachiller R, Chapillon E, Gueth F, Gusdorf A, Lefloch B, Leurini S, Pineau des Forêts G, Rygl KLJ, Tafalla M (2018) Water and interstellar complex organics associated with the HH 212 protostellar disc.

On disc atmospheres, disc winds, and accretion shocks. A&A617:A10, DOI 10.1051/0004-6361/201832765, 1806.07967

Codella C, Ceccarelli C, Lee CF, Bianchi E, Balucani N, Podio L, Cabrit S, Gueth F, Gusdorf A, Lefloch B, Tabone B (2019) The HH 212 Interstellar Laboratory: Astrochemistry as a Tool To Reveal Protostellar Disks on Solar System Scales around a Rising Sun. ACS Earth and Space Chemistry 3(10):2110–2121, DOI 10.1021/acsearthspacechem.9b00136, 1910.04442

Codella C, Podio L, Garufi A, Perrero J, Ugliengo P, Fedele D, Favre C, Bianchi E, Ceccarelli C, Mercimek S, Bacciotti F, Rygl KLJ, Testi L (2020) ALMA chemical survey of disk-outflow sources in Taurus (ALMA-DOT). IV. Thioformaldehyde (H_2CS) in protoplanetary disks: spatial distributions and binding energies. arXiv e-prints arXiv:2011.02305, 2011.02305

Côté B, O'Shea BW, Ritter C, Herwig F, Venn KA (2017) The Impact of Modeling Assumptions in Galactic Chemical Evolution Models. ApJ835(2):128, DOI 10.3847/1538-4357/835/2/128, 1604.07824

Côté B, Eichler M, Arcones A, Hansen CJ, Simonetti P, Frebel A, Fryer CL, Pignatari M, Reichert M, Belczynski K, Matteucci F (2019a) Neutron Star Mergers Might Not Be the Only Source of r-process Elements in the Milky Way. ApJ875(2):106, DOI 10.3847/1538-4357/ab10db, 1809.03525

Côté B, Lugaro M, Reifarth R, Pignatari M, Világos B, Yagüe A, Gibson BK (2019b) Galactic Chemical Evolution of Radioactive Isotopes. ApJ878(2):156, DOI 10.3847/1538-4357/ab21d1, 1905.07828

Côté B, Yagüe A, Világos B, Lugaro M (2019c) Stochastic Chemical Evolution of Radioactive Isotopes with a Monte Carlo Approach. ApJ887(2):213, DOI 10.3847/1538-4357/ab5a88

Cowan JJ, Sneden C, Lawler JE, Aprahamian A, Wiescher M, Langanke K, Martínez-Pinedo G, Thielemann FK (2019) Making the Heaviest Elements in the Universe: A Review of the Rapid Neutron Capture Process. arXiv e-prints arXiv:1901.01410, 1901.01410

Cridland AJ, van Dishoeck EF, Alessi M, Pudritz RE (2019) Connecting planet formation and astrochemistry. A main sequence for C/O in hot exoplanetary atmospheres. A&A632:A63, DOI 10.1051/0004-6361/201936105, 1910.13171

da Silva R, Milone AC, Reddy BE (2011) Homogeneous photospheric parameters and C abundances in G and K nearby stars with and without planets. A&A526:A71, DOI 10.1051/0004-6361/201015907, 1011.5768

D'Alessio P, Calvet N, Hartmann L (2001) Accretion Disks around Young Objects. III. Grain Growth. ApJ553(1):321–334, DOI 10.1086/320655, astro-ph/0101443

D'Angelo G, Lissauer JJ (2018) Formation of Giant Planets, p 140. DOI 10.1007/978-3-319-55333-7_140

Dartois E, Dutrey A, Guilloteau S (2003) Structure of the DM Tau Outer Disk: Probing the vertical kinetic temperature gradient. A&A399:773–787, DOI 10.1051/0004-6361:20021638

Davies MB, Adams FC, Armitage P, Chambers J, Ford E, Morbidelli A, Raymond SN, Veras D (2014) The Long-Term Dynamical Evolution of

Planetary Systems. In: Beuther H, Klessen RS, Dullemond CP, Henning T (eds) Protostars and Planets VI, p 787, DOI 10.2458/azu_uapress_9780816531240-ch034, `1311.6816`

de Juan Ovelar M, Kruijssen JMD, Bressert E, Testi L, Bastian N, Cánovas H (2012) Can habitable planets form in clustered environments? A&A546:L1, DOI 10.1051/0004-6361/201219627, `1209.2136`

Delgado Mena E, Israelian G, González Hernández JI, Bond JC, Santos NC, Udry S, Mayor M (2010) Chemical Clues on the Formation of Planetary Systems: C/O Versus Mg/Si for HARPS GTO Sample. ApJ725(2):2349–2358, DOI 10.1088/0004-637X/725/2/2349, `1009.5224`

Delgado Mena E, Israelian G, González Hernández JI, Santos NC, Rebolo R (2012) Be Abundances in Cool Main-sequence Stars with Exoplanets. ApJ746(1):47, DOI 10.1088/0004-637X/746/1/47, `1111.3495`

Delgado Mena E, Israelian G, González Hernández JI, Sousa SG, Mortier A, Santos NC, Adibekyan VZ, Fernand es J, Rebolo R, Udry S, Mayor M (2014) Li depletion in solar analogues with exoplanets. Extending the sample. A&A562:A92, DOI 10.1051/0004-6361/201321493, `1311.6414`

Delgado Mena E, Bertrán de Lis S, Adibekyan VZ, Sousa SG, Figueira P, Mortier A, González Hernández JI, Tsantaki M, Israelian G, Santos NC (2015) Li abundances in F stars: planets, rotation, and Galactic evolution. A&A576:A69, DOI 10.1051/0004-6361/201425433, `1412.4618`

Dominik C, Habing H (2000) Old and Young Vega-like Stars. In: Astronomische Gesellschaft Meeting Abstracts, Astronomische Gesellschaft Meeting Abstracts, vol 17

Doyle AE, Young ED, Klein B, Zuckerman B, Schlichting HE (2019) Oxygen fugacities of extrasolar rocks: Evidence for an Earth-like geochemistry of exoplanets. Science 366(6463):356–359, DOI 10.1126/science.aax3901, `1910.12989`

Drozdovskaya MN, van Dishoeck EF, Rubin M, Jørgensen JK, Altwegg K (2019) Ingredients for solar-like systems: protostar IRAS 16293-2422 B versus comet 67P/Churyumov-Gerasimenko. MNRAS490(1):50–79, DOI 10.1093/\mnras/stz2430, `1908.11290`

Du F, Bergin EA, Hogerheijde MR (2015) Volatile depletion in the TW Hydrae disk atmosphere. ApJ807(2):L32, DOI 10.1088/2041-8205/807/2/L32, `1506.03510`

Du F, Bergin EA, Hogerheijde M, van Dishoeck EF, Blake G, Bruderer S, Cleeves I, Dominik C, Fedele D, Lis DC, Melnick G, Neufeld D, Pearson J, Yıldız U (2017) Survey of Cold Water Lines in Protoplanetary Disks: Indications of Systematic Volatile Depletion. ApJ842(2):98, DOI 10.3847/1538-4357/aa70ee, `1705.00799`

Dumusque X, Pepe F, Lovis C, Ségransan D, Sahlmann J, Benz W, Bouchy F, Mayor M, Queloz D, Santos N, Udry S (2012) An Earth-mass planet orbiting α Centauri B. Nature491(7423):207–211, DOI 10.1038/nature11572

Dutrey A, Guilloteau S, Duvert G, Prato L, Simon M, Schuster K, Menard F (1996) Dust and gas distribution around T Tauri stars in Taurus-Auriga. I. Interferometric 2.7mm continuum and $\hat{1}$3ĈO J=1-0 observations.

A&A309:493–504

Dutrey A, Wakelam V, Boehler Y, Guilloteau S, Hersant F, Semenov D, Chapillon E, Henning T, Piétu V, Launhardt R, Gueth F, Schreyer K (2011) Chemistry in disks. V. Sulfur-bearing molecules in the protoplanetary disks surrounding LkCa15, MWC480, DM Tauri, and GO Tauri. A&A535:A104, DOI 10.1051/0004-6361/201116931, `1109.5870`

Ecuvillon A, Israelian G, Santos NC, Mayor M, Villar V, Bihain G (2004) C, S, Zn and Cu abundances in planet-harbouring stars. A&A426:619–630, DOI 10.1051/0004-6361:20041136, `astro-ph/0406584`

Ecuvillon A, Israelian G, Santos NC, Mayor M, Gilli G (2006) Abundance ratios of volatile vs. refractory elements in planet-harbouring stars: hints of pollution? A&A449(2):809–816, DOI 10.1051/0004-6361:20054534, `astro-ph/0512221`

Edwards B, Mugnai L, Tinetti G, Pascale E, Sarkar S (2019) An Updated Study of Potential Targets for Ariel. AJ157(6):242, DOI 10.3847/1538-3881/ab1cb9, `1905.04959`

Eistrup C, Walsh C, van Dishoeck EF (2016) Setting the volatile composition of (exo)planet-building material. Does chemical evolution in disk midplanes matter? A&A595:A83, DOI 10.1051/0004-6361/201628509, `1607.06710`

Eistrup C, Walsh C, van Dishoeck EF (2018) Molecular abundances and C/O ratios in chemically evolving planet-forming disk midplanes. A&A613:A14, DOI 10.1051/0004-6361/201731302, `1709.07863`

Elmegreen BG, Falgarone E (1996) A Fractal Origin for the Mass Spectrum of Interstellar Clouds. ApJ471:816, DOI 10.1086/178009

Favre C, Cleeves LI, Bergin EA, Qi C, Blake GA (2013) A Significantly Low CO Abundance toward the TW Hya Protoplanetary Disk: A Path to Active Carbon Chemistry? ApJ776(2):L38, DOI 10.1088/2041-8205/776/2/L38, `1309.5370`

Favre C, Fedele D, Semenov D, Parfenov S, Codella C, Ceccarelli C, Bergin EA, Chapillon E, Testi L, Hersant F, Lefloch B, Fontani F, Blake GA, Cleeves LI, Qi C, Schwarz KR, Taquet V (2018) First Detection of the Simplest Organic Acid in a Protoplanetary Disk. ApJ862(1):L2, DOI 10.3847/2041-8213/aad046, `1807.05768`

Fedele D, Pascucci I, Brittain S, Kamp I, Woitke P, Williams JP, Dent WRF, Thi WF (2011) Water Depletion in the Disk Atmosphere of Herbig AeBe Stars. ApJ732(2):106, DOI 10.1088/0004-637X/732/2/106, `1103.6039`

Fedele D, Bruderer S, van Dishoeck EF, Herczeg GJ, Evans NJ, Bouwman J, Henning T, Green J (2012) Warm H_2O and OH in the disk around the Herbig star HD 163296. A&A544:L9, DOI 10.1051/0004-6361/201219615, `1207.3969`

Fedele D, Bruderer S, van Dishoeck EF, Carr J, Herczeg GJ, Salyk C, Evans NJ, Bouwman J, Meeus G, Henning T, Green J, Najita JR, Güdel M (2013) DIGIT survey of far-infrared lines from protoplanetary disks. I. [O i], [C ii], OH, H_2O, and CH^+. A&A559:A77, DOI 10.1051/0004-6361/201321118, `1308.1578`

Fedele D, van Dishoeck EF, Kama M, Bruderer S, Hogerheijde MR (2016) Probing the 2D temperature structure of protoplanetary disks with Herschel observations of high-J CO lines. A&A591:A95, DOI 10.1051/0004-6361/201526948, 1604.02055

Fedele D, Carney M, Hogerheijde MR, Walsh C, Miotello A, Klaassen P, Bruderer S, Henning T, van Dishoeck EF (2017) ALMA unveils rings and gaps in the protoplanetary system ¡ASTROBJ¿HD 169142¡/ASTROBJ¿: signatures of two giant protoplanets. A&A600:A72, DOI 10.1051/0004-6361/201629860, 1702.02844

Fedele D, Tazzari M, Booth R, Testi L, Clarke CJ, Pascucci I, Kospal A, Semenov D, Bruderer S, Henning T, Teague R (2018) ALMA continuum observations of the protoplanetary disk AS 209. Evidence of multiple gaps opened by a single planet. A&A610:A24, DOI 10.1051/0004-6361/201731978, 1711.05185

Fischer DA, Valenti J (2005) The Planet-Metallicity Correlation. ApJ622(2):1102–1117, DOI 10.1086/428383

Fujimoto Y, Krumholz MR, Tachibana S (2018) Short-lived radioisotopes in meteorites from Galactic-scale correlated star formation. MNRAS480(3):4025–4039, DOI 10.1093/mnras/sty2132, 1802.08695

Fulle M, Blum J, Green SF, Gundlach B, Herique A, Moreno F, Mottola S, Rotundi A, Snodgrass C (2019) The refractory-to-ice mass ratio in comets. MNRAS482(3):3326–3340, DOI 10.1093/\mnras/sty2926

Garufi A, Podio L, Codella C, Fedele D, Bianchi E, Favre C, Bacciotti F, Ceccarelli C, Mercimek S, Rygl K, Teague R, Testi L (2020a) ALMA chemical survey of disk-outflow sources in Taurus (ALMA-DOT) V: Sample, overview, and demography of disk molecular emission. arXiv e-prints arXiv:2012.07667, 2012.07667

Garufi A, Podio L, Codella C, Rygl K, Bacciotti F, Facchini S, Fedele D, Miotello A, Teague R, Testi L (2020b) ALMA chemical survey of disk-outflow sources in Taurus (ALMA-DOT): I. CO, CS, CN, and H2CO around DG Tau B. arXiv e-prints arXiv:2002.10195, 2002.10195

Ghezzi L, Cunha K, Smith VV, de la Reza R (2010) Lithium Abundances in a Sample of Planet-hosting Dwarfs. ApJ724(1):154–164, DOI 10.1088/0004-637X/724/1/154, 1009.2130

Gibb EL, Horne D (2013) Detection of CH_4 in the GV Tau N Protoplanetary Disk. ApJ776(2):L28, DOI 10.1088/2041-8205/776/2/L28

Gieles M, Portegies Zwart SF (2011) The distinction between star clusters and associations. MNRAS410(1):L6–L7, DOI 10.1111/j.1745-3933.2010.00967.x, 1010.1720

Gilli G, Israelian G, Ecuvillon A, Santos NC, Mayor M (2006) Abundances of refractory elements in the atmospheres of stars with extrasolar planets. A&A449(2):723–736, DOI 10.1051/0004-6361:20053850, astro-ph/0512219

Gonzalez G (1997) The stellar metallicity-giant planet connection. MNRAS285(2):403–412, DOI 10.1093/\mnras/285.2.403

Gonzalez G (2006) The Chemical Compositions of Stars with Planets: A Review. PASP118(849):1494–1505, DOI 10.1086/509792, `astro-ph/0609829`

Gonzalez G (2008) Parent stars of extrasolar planets - IX. Lithium abundances. MNRAS386(2):928–934, DOI 10.1111/j.1365-2966.2008.13067.x, `0802.0434`

Gonzalez G (2009) Stars with planets and the thick disc. MNRAS399:L103–L107, DOI 10.1111/j.1745-3933.2009.00734.x

Gonzalez G (2011) Parent stars of extrasolar planets - XII. Additional evidence for trends with v sin i, condensation temperature and chromospheric activity. MNRAS416(1):L80–L83, DOI 10.1111/j.1745-3933.2011.01102.x, `1106.5002`

Gonzalez G, Carlson MK, Tobin RW (2010) Parent stars of extrasolar planets - XI. Trends with condensation temperature revisited. MNRAS407(1):314–320, DOI 10.1111/j.1365-2966.2010.16900.x, `1004.3313`

González Hernández JI, Israelian G, Santos NC, Sousa S, Delgado-Mena E, Neves V, Udry S (2010) Searching for the Signatures of Terrestrial Planets in Solar Analogs. ApJ720(2):1592–1602, DOI 10.1088/0004-637X/720/2/1592, `1007.0580`

González Hernández JI, Delgado-Mena E, Sousa SG, Israelian G, Santos NC, Adibekyan VZ, Udry S (2013) Searching for the signatures of terrestrial planets in F-, G-type main-sequence stars. A&A552:A6, DOI 10.1051/0004-6361/201220165, `1301.2109`

Guarcello MG, Drake JJ, Wright NJ, Albacete-Colombo JF, Clarke C, Ercolano B, Flaccomio E, Kashyap V, Micela G, Naylor T, Schneider N, Sciortino S, Vink JS (2016) Photoevaporation and close encounters: how the environment around Cygnus OB2 affects the evolution of protoplanetary disks. arXiv e-prints arXiv:1605.01773, `1605.01773`

Guilloteau S, Di Folco E, Dutrey A, Simon M, Grosso N, Piétu V (2013) A sensitive survey for ^{13}CO, CN, H_2CO, and SO in the disks of T Tauri and Herbig Ae stars. A&A549:A92, DOI 10.1051/0004-6361/201220298, `1211.4776`

Guilloteau S, Reboussin L, Dutrey A, Chapillon E, Wakelam V, Piétu V, Di Folco E, Semenov D, Henning T (2016) Chemistry in disks. X. The molecular content of protoplanetary disks in Taurus. A&A592:A124, DOI 10.1051/0004-6361/201527088, `1604.05028`

Haworth TJ, Clarke CJ, Rahman W, Winter AJ, Facchini S (2018) The FRIED grid of mass-loss rates for externally irradiated protoplanetary discs. MNRAS481(1):452–466, DOI 10.1093/\mnras/sty2323, `1808.07484`

Haywood M (2008) A peculiarity of metal-poor stars with planets? A&A482(2):673–676, DOI 10.1051/0004-6361:20079141, `0804.2954`

He MY, Ford EB, Ragozzine D, Carrera D (2020) Architectures of Exoplanetary Systems. III. Eccentricity and Mutual Inclination Distributions of AMD-stable Planetary Systems. AJ160(6):276, DOI 10.3847/1538-3881/abba18, `2007.14473`

Helled R, Bodenheimer P, Podolak M, Boley A, Meru F, Nayakshin S, Fortney JJ, Mayer L, Alibert Y, Boss AP (2014) Giant Planet Formation, Evolution, and Internal Structure. In: Beuther H, Klessen RS, Dulle-

mond CP, Henning T (eds) Protostars and Planets VI, p 643, DOI 10.2458/azu_uapress_9780816531240-ch028, `1311.1142`

Hogerheijde MR, Bergin EA, Brinch C, Cleeves LI, Fogel JKJ, Blake GA, Dominik C, Lis DC, Melnick G, Neufeld D, Panić O, Pearson JC, Kristensen L, Yıldız UA, van Dishoeck EF (2011) Detection of the Water Reservoir in a Forming Planetary System. Science 334(6054):338, DOI 10.1126/science.1208931, `1110.4600`

Hopkins PF (2013) Why do stars form in clusters? An analytic model for stellar correlation functions. MNRAS428(3):1950–1957, DOI 10.1093/\mnras/sts147, `1202.2122`

Ikoma M, Genda H (2006) Constraints on the Mass of a Habitable Planet with Water of Nebular Origin. ApJ 648(1):696–706, DOI 10.1086/505780, `astro-ph/0606117`

Ikoma M, Elkins-Tanton L, Hamano K, Suckale J (2018) Water Partitioning in Planetary Embryos and Protoplanets with Magma Oceans. SSRv 214(4):76, DOI 10.1007/s11214-018-0508-3, `1804.09294`

Isaacson H, Fischer D (2010) Chromospheric Activity and Jitter Measurements for 2630 Stars on the California Planet Search. ApJ725(1):875–885, DOI 10.1088/0004-637X/725/1/875, `1009.2301`

Isella A, Hull CLH, Moullet A, Galván-Madrid R, Johnstone D, Ricci L, Tobin J, Testi L, Beltran M, Lazio J, Siemion A, Liu HB, Du F, Öberg KI, Bergin T, Caselli P, Bourke T, Carilli C, Perez L, Butler B, de Pater I, Qi C, Hofstadter M, Moreno R, Alexander D, Williams J, Goldsmith P, Wyatt M, Loinard L, Di Francesco J, Wilner D, Schilke P, Ginsburg A, Sánchez-Monge Á, Zhang Q, Beuther H (2015) Next Generation Very Large Array Memo No. 6, Science Working Group 1: The Cradle of Life. arXiv e-prints arXiv:1510.06444, `1510.06444`

Isella A, Guidi G, Testi L, Liu S, Li H, Li S, Weaver E, Boehler Y, Carperter JM, De Gregorio-Monsalvo I, Manara CF, Natta A, Pérez LM, Ricci L, Sargent A, Tazzari M, Turner N (2016) Ringed Structures of the HD 163296 Protoplanetary Disk Revealed by ALMA. Phys. Rev. Lett.117(25):251101, DOI 10.1103/PhysRevLett.117.251101

Isnard R, Bardyn A, Fray N, Briois C, Cottin H, Paquette J, Stenzel O, Alexander C, Baklouti D, Engrand C, Orthous-Daunay FR, Siljeström S, Varmuza K, Hilchenbach M (2019) H/C elemental ratio of the refractory organic matter in cometary particles of 67P/Churyumov-Gerasimenko. A&A630:A27, DOI 10.1051/0004-6361/201834797

Israelian G, Santos NC, Mayor M, Rebolo R (2004) Lithium in stars with exoplanets. A&A414:601–611, DOI 10.1051/0004-6361:20034398, `astro-ph/0310378`

Jenkins JS, Jones HRA, Tuomi M, Díaz M, Cordero JP, Aguayo A, Pantoja B, Arriagada P, Mahu R, Brahm R, Rojo P, Soto MG, Ivanyuk O, Becerra Yoma N, Day-Jones AC, Ruiz MT, Pavlenko YV, Barnes JR, Murgas F, Pinfield DJ, Jones MI, López-Morales M, Shectman S, Butler RP, Minniti D (2017) New planetary systems from the Calan-Hertfordshire Extrasolar Planet Search. MNRAS466:443–473, DOI 10.1093/\mnras/stw2811, `1603.`

      09391

Jermyn AS, Kama M (2018) Stellar photospheric abundances as a probe of
      discs and planets. MNRAS476(4):4418–4434, DOI 10.1093/\mnras/sty429,
      1804.06414

Jofré E, Petrucci R, Saffe C, Saker L, de la Villarmois EA, Chavero C,
      Gómez M, Mauas PJD (2015) Stellar parameters and chemical abun-
      dances of 223 evolved stars with and without planets. A&A574:A50, DOI
      10.1051/0004-6361/201424474, 1410.6422

Johnson JA, Aller KM, Howard AW, Crepp JR (2010) Giant Planet Oc-
      currence in the Stellar Mass-Metallicity Plane. PASP122(894):905, DOI
      10.1086/655775, 1005.3084

Johnson TV, Mousis O, Lunine JI, Madhusudhan N (2012) Planetesimal Com-
      positions in Exoplanet Systems. ApJ757(2):192, DOI 10.1088/0004-637X/
      757/2/192, 1208.3289

Jones SW, Möller H, Fryer CL, Fontes CJ, Trappitsch R, Even WP, Couture
      A, Mumpower MR, Safi-Harb S (2019) ^{60}Fe in core-collapse supernovae
      and prospects for X-ray and gamma-ray detection in supernova remnants.
      MNRAS485(3):4287–4310, DOI 10.1093/\mnras/stz536, 1902.05980

Kama M, Folsom CP, Pinilla P (2015) Fingerprints of giant planets in the pho-
      tospheres of Herbig stars. A&A582:L10, DOI 10.1051/0004-6361/201527094,
      1509.02741

Kama M, Bruderer S, Carney M, Hogerheijde M, van Dishoeck EF, Fedele
      D, Baryshev A, Boland W, Güsten R, Aikutalp A, Choi Y, Endo A,
      Frieswijk W, Karska A, Klaassen P, Koumpia E, Kristensen L, Leurini
      S, Nagy Z, Perez Beaupuits JP, Risacher C, van der Marel N, van Kem-
      pen TA, van Weeren RJ, Wyrowski F, Yıldız UA (2016a) Observations
      and modelling of CO and [C I] in protoplanetary disks. First detections
      of [C I] and constraints on the carbon abundance. A&A588:A108, DOI
      10.1051/0004-6361/201526791, 1601.01449

Kama M, Bruderer S, van Dishoeck EF, Hogerheijde M, Folsom CP, Miotello
      A, Fedele D, Belloche A, Güsten R, Wyrowski F (2016b) Volatile-carbon
      locking and release in protoplanetary disks. A study of TW Hya and HD
      100546. A&A592:A83, DOI 10.1051/0004-6361/201526991, 1605.05093

Kama M, Shorttle O, Jermyn AS, Folsom CP, Furuya K, Bergin EA, Walsh
      C, Keller L (2019) Abundant Refractory Sulfur in Protoplanetary Disks.
      ApJ885(2):114, DOI 10.3847/1538-4357/ab45f8, 1908.05169

Kama M, Trapman L, Fedele D, Bruderer S, Hogerheijde MR, Miotello A, van
      Dishoeck EF, Clarke C, Bergin EA (2020) Mass constraints for 15 protoplan-
      etary discs from HD 1-0. A&A634:A88, DOI 10.1051/0004-6361/201937124,
      1912.11883

Kashyap VL, Drake JJ, Saar SH (2008) Extrasolar Giant Planets and X-Ray
      Activity. ApJ687(2):1339–1354, DOI 10.1086/591922, 0807.1308

Kennicutt RC, Evans NJ (2012) Star Formation in the Milky Way and Nearby
      Galaxies. ARA&A50:531–608, DOI 10.1146/annurev-astro-081811-125610,
      1204.3552

Kimura T, Ikoma M (2020) Formation of aqua planets with water of nebular origin: effects of water enrichment on the structure and mass of captured atmospheres of terrestrial planets. MNRAS496(3):3755–3766, DOI 10.1093/mnras/staa1778, 2006.09068

Kobayashi C, Karakas AI, Umeda H (2011) The evolution of isotope ratios in the Milky Way Galaxy. MNRAS414(4):3231–3250, DOI 10.1111/j.1365-2966.2011.18621.x, 1102.5312

Koll D, Korschinek G, Faestermann T, Gómez-Guzmán JM, Kipfstuhl S, Merchel S, Welch JM (2019) Interstellar ^{60}Fe in Antarctica. Phys. Rev. Lett.123(7):072701, DOI 10.1103/PhysRevLett.123.072701

Krijt S, Schwarz KR, Bergin EA, Ciesla FJ (2018) Transport of CO in Protoplanetary Disks: Consequences of Pebble Formation, Settling, and Radial Drift. ApJ864(1):78, DOI 10.3847/1538-4357/aad69b, 1808.01840

Kruijssen JMD (2012) On the fraction of star formation occurring in bound stellar clusters. MNRAS426(4):3008–3040, DOI 10.1111/j.1365-2966.2012.21923.x, 1208.2963

Kruijssen JMD, Longmore SN (2020) The implications of clustered star formation for (proto)planetary systems and habitability. In: Elmegreen BG, Tóth LV, Güdel M (eds) IAU Symposium, IAU Symposium, vol 345, pp 61–65, DOI 10.1017/S1743921319001686, 1901.04491

Kruijssen JMD, Longmore SN, Chevance M (2020) Bridging the Planet Radius Valley: Stellar Clustering as a Key Driver for Turning Sub-Neptunes into Super-Earths. arXiv e-prints arXiv:2011.11680, 2011.11680

Krumholz MR, McKee CF (2005) A General Theory of Turbulence-regulated Star Formation, from Spirals to Ultraluminous Infrared Galaxies. ApJ630(1):250–268, DOI 10.1086/431734, astro-ph/0505177

Lada CJ (1987) Star formation: from OB associations to protostars. In: Peimbert M, Jugaku J (eds) Star Forming Regions, IAU Symposium, vol 115, p 1

Lada CJ, Lada EA (2003) Embedded Clusters in Molecular Clouds. ARA&A41:57–115, DOI 10.1146/annurev.astro.41.011802.094844, astro-ph/0301540

Laskar J, Petit AC (2017) AMD-stability and the classification of planetary systems. A&A605:A72, DOI 10.1051/0004-6361/201630022, 1703.07125

Le Gal R, Öberg KI, Loomis RA, Pegues J, Bergner JB (2019) Sulfur Chemistry in Protoplanetary Disks: CS and H_2CS. ApJ876(1):72, DOI 10.3847/1538-4357/ab1416, 1903.11105

Lee CF, Li ZY, Ho PTP, Hirano N, Zhang Q, Shang H (2017) Formation and Atmosphere of Complex Organic Molecules of the HH 212 Protostellar Disk. ApJ843(1):27, DOI 10.3847/1538-4357/aa7757, 1706.06041

Lee CF, Codella C, Li ZY, Liu SY (2019a) First Abundance Measurement of Organic Molecules in the Atmosphere of HH 212 Protostellar Disk. ApJ876(1):63, DOI 10.3847/1538-4357/ab15db, 1904.10572

Lee JE, Lee S, Baek G, Aikawa Y, Cieza L, Yoon SY, Herczeg G, Johnstone D, Casassus S (2019b) The ice composition in the disk around V883 Ori revealed by its stellar outburst. Nature Astronomy 3:314–319, DOI 10.1038/

s41550-018-0680-0, `1809.00353`

Limbach MA, Turner EL (2015) Exoplanet orbital eccentricity: Multiplicity relation and the Solar System. Proceedings of the National Academy of Science 112(1):20–24, DOI 10.1073/pnas.1406545111, `1404.2552`

Limongi M, Chieffi A (2006) The Nucleosynthesis of ^{26}Al and ^{60}Fe in Solar Metallicity Stars Extending in Mass from 11 to 120 M$_{solar}$: The Hydrostatic and Explosive Contributions. ApJ647(1):483–500, DOI 10.1086/505164, `astro-ph/0604297`

Lodders K (2003) Solar System Abundances and Condensation Temperatures of the Elements. ApJ591:1220–1247, DOI 10.1086/375492

Lodders K (2010a) Exoplanet Chemistry, p 157. DOI 10.1002/9783527629763. ch8

Lodders K (2010b) Solar System Abundances of the Elements. Astrophysics and Space Science Proceedings 16:379, DOI 10.1007/978-3-642-10352-0_8, `1010.2746`

Lodders K (2019) Solar Elemental Abundances. arXiv e-prints arXiv:1912.00844, `1912.00844`

Long F, Pinilla P, Herczeg GJ, Harsono D, Dipierro G, Pascucci I, Hendler N, Tazzari M, Ragusa E, Salyk C, Edwards S, Lodato G, van de Plas G, Johnstone D, Liu Y, Boehler Y, Cabrit S, Manara CF, Menard F, Mulders GD, Nisini B, Fischer WJ, Rigliaco E, Banzatti A, Avenhaus H, Gully-Santiago M (2018) Gaps and Rings in an ALMA Survey of Disks in the Taurus Star-forming Region. ApJ869(1):17, DOI 10.3847/1538-4357/aae8e1, `1810.06044`

Longmore SN, Kruijssen JMD, Bastian N, Bally J, Rathborne J, Testi L, Stolte A, Dale J, Bressert E, Alves J (2014) The Formation and Early Evolution of Young Massive Clusters. In: Beuther H, Klessen RS, Dullemond CP, Henning T (eds) Protostars and Planets VI, p 291, DOI 10.2458/azu_uapress_9780816531240-ch013, `1401.4175`

Longmore SN, Chevance M, Kruijssen JMD (2021) The Impact of Stellar Clustering on the Observed Architectures of Planetary Systems. ApJ submitted

Loomis RA, Cleeves LI, Öberg KI, Guzman VV, Andrews SM (2015) The Distribution and Chemistry of H_2CO in the DM Tau Protoplanetary Disk. ApJ809(2):L25, DOI 10.1088/2041-8205/809/2/L25, `1508.07004`

Loomis RA, Öberg KI, Andrews SM, Bergin E, Bergner J, Blake GA, Cleeves LI, Czekala I, Huang J, Le Gal R, Ménard F, Pegues J, Qi C, Walsh C, Williams JP, Wilner DJ (2020) An Unbiased ALMA Spectral Survey of the LkCa 15 and MWC 480 Protoplanetary Disks. ApJ893(2):101, DOI 10.3847/1538-4357/ab7cc8

Ludwig P, Bishop S, Egli R, Chernenko V, Deneva B, Faestermann T, Famulok N, Fimiani L, Gómez-Guzmán JM, Hain K, Korschinek G, Hanzlik M, Merchel S, Rugel G (2016) Time-resolved 2-million-year-old supernova activity discovered in Earth's microfossil record. Proceedings of the National Academy of Science 113(33):9232–9237, DOI 10.1073/pnas.1601040113, `1710.09573`

Lugaro M, Ott U, Kereszturi Á (2018) Radioactive nuclei from cosmochronology to habitability. Progress in Particle and Nuclear Physics 102:1–47, DOI 10.1016/j.ppnp.2018.05.002, 1808.00233

Ma B, Ge J (2014) Statistical properties of brown dwarf companions: implications for different formation mechanisms. MNRAS439:2781–2789, DOI 10.1093/\mnras/stu134, 1303.6442

Madhusudhan N (2019) Exoplanetary Atmospheres: Key Insights, Challenges, and Prospects. ARA&A57:617–663, DOI 10.1146/annurev-astro-081817-051846, 1904.03190

Madhusudhan N, Agúndez M, Moses JI, Hu Y (2016) Exoplanetary Atmospheres—Chemistry, Formation Conditions, and Habitability. Space Sci. Rev.205(1-4):285–348, DOI 10.1007/s11214-016-0254-3, 1604.06092

Maggio A, Pillitteri I, Scandariato G, Lanza AF, Sciortino S, Borsa F, Bonomo AS, Claudi R, Covino E, Desidera S, Gratton R, Micela G, Pagano I, Piotto G, Sozzetti A, Cosentino R, Maldonado J (2015) Coordinated X-Ray and Optical Observations of Star-Planet Interaction in HD 17156. ApJ811(1):L2, DOI 10.1088/2041-8205/811/1/L2, 1509.00662

Maldonado J, Villaver E (2016) Evolved stars and the origin of abundance trends in planet hosts. A&A588:A98, DOI 10.1051/0004-6361/201527883, 1602.00835

Maldonado J, Villaver E (2017) Searching for chemical signatures of brown dwarf formation. A&A602:A38, DOI 10.1051/0004-6361/201630120, 1702.02904

Maldonado J, Villaver E, Eiroa C (2013) The metallicity signature of evolved stars with planets. A&A554:A84, DOI 10.1051/0004-6361/201321082, 1303.3418

Maldonado J, Eiroa C, Villaver E, Montesinos B, Mora A (2015) Searching for signatures of planet formation in stars with circumstellar debris discs. A&A579:A20, DOI 10.1051/0004-6361/201525764, 1502.07100

Maldonado J, Villaver E, Eiroa C (2018) Chemical fingerprints of hot Jupiter planet formation. A&A612:A93, DOI 10.1051/0004-6361/201732001, 1712.01035

Maldonado J, Villaver E, Eiroa C, Micela G (2019) Connecting substellar and stellar formation: the role of the host star's metallicity. A&A624:A94, DOI 10.1051/0004-6361/201833827, 1903.01141

Manara CF, Morbidelli A, Guillot T (2018) Why do protoplanetary disks appear not massive enough to form the known exoplanet population? A&A618:L3, DOI 10.1051/0004-6361/201834076, 1809.07374

Mandell AM, Mumma MJ, Blake GA, Bonev BP, Villanueva GL, Salyk C (2008) Discovery of OH in Circumstellar Disks around Young Intermediate-Mass Stars. ApJ681(1):L25, DOI 10.1086/590180, 0805.3502

Mandell AM, Bast J, van Dishoeck EF, Blake GA, Salyk C, Mumma MJ, Villanueva G (2012) First Detection of Near-infrared Line Emission from Organics in Young Circumstellar Disks. ApJ747(2):92, DOI 10.1088/0004-637X/747/2/92, 1201.0766

Marboeuf U, Thiabaud A, Alibert Y, Cabral N, Benz W (2014a) From planetesimals to planets: volatile molecules. A&A570:A36, DOI 10.1051/0004-6361/201423431, 1407.7282

Marboeuf U, Thiabaud A, Alibert Y, Cabral N, Benz W (2014b) From stellar nebula to planetesimals. A&A570:A35, DOI 10.1051/0004-6361/201322207, 1407.7271

Marzari F, Picogna G (2013) Circumstellar disks do erase the effects of stellar flybys on planetary systems. A&A550:A64, DOI 10.1051/0004-6361/201220436, 1212.1561

Matthews B, Kennedy G, Sibthorpe B, Booth M, Wyatt M, Broekhoven-Fiene H, Macintosh B, Marois C (2014) Resolved Imaging of the HR 8799 Debris Disk with Herschel. ApJ780(1):97, DOI 10.1088/0004-637X/780/1/97, 1311.2977

Mayor M, Marmier M, Lovis C, Udry S, Ségransan D, Pepe F, Benz W, Bertaux J, Bouchy F, Dumusque X, Lo Curto G, Mordasini C, Queloz D, Santos NC (2011) The HARPS search for southern extra-solar planets XXXIV. Occurrence, mass distribution and orbital properties of super-Earths and Neptune-mass planets. ArXiv e-prints 1109.2497

McClure MK (2019) Carbon depletion observed inside T Tauri inner rims. Formation of icy, kilometer size planetesimals by 1 Myr. A&A632:A32, DOI 10.1051/0004-6361/201834361, 1910.06029

McClure MK, Bergin EA, Cleeves LI, van Dishoeck EF, Blake GA, Evans I N J, Green JD, Henning T, Öberg KI, Pontoppidan KM, Salyk C (2016) Mass Measurements in Protoplanetary Disks from Hydrogen Deuteride. ApJ831(2):167, DOI 10.3847/0004-637X/831/2/167, 1608.07817

Meléndez J, Asplund M, Gustafsson B, Yong D (2009) The Peculiar Solar Composition and Its Possible Relation to Planet Formation. ApJ704(1):L66–L70, DOI 10.1088/0004-637X/704/1/L66, 0909.2299

Melott AL, Marinho F, Paulucci L (2019) Hypothesis: Muon Radiation Dose and Marine Megafaunal Extinction at the End-Pliocene Supernova. Astrobiology 19(6):825–830, DOI 10.1089/ast.2018.1902, 1712.09367

Mendigutía I, Calvet N, Montesinos B, Mora A, Muzerolle J, Eiroa C, Oudmaijer RD, Merín B (2011) Accretion rates and accretion tracers of Herbig Ae/Be stars. A&A535:A99, DOI 10.1051/0004-6361/201117444, 1109.3288

Mendigutía I, Mora A, Montesinos B, Eiroa C, Meeus G, Merín B, Oudmaijer RD (2012) Accretion-related properties of Herbig Ae/Be stars. Comparison with T Tauris. A&A543:A59, DOI 10.1051/0004-6361/201219110, 1205.4734

Miguel Y, Kaltenegger L, Fegley B, Schaefer L (2011) Compositions of Hot Super-earth Atmospheres: Exploring Kepler Candidates. ApJ742(2):L19, DOI 10.1088/2041-8205/742/2/L19, 1110.2426

Miguel Y, Cridland A, Ormel CW, Fortney JJ, Ida S (2019) Diverse outcomes of planet formation and composition around low-mass stars and brown dwarfs. MNRASp 2610, DOI 10.1093/\mnras/stz3007, 1909.12320

Miley JM, Panić O, Wyatt M, Kennedy GM (2018) Unlocking the secrets of the midplane gas and dust distribution in the young hybrid disc HD 141569.

A&A615:L10, DOI 10.1051/0004-6361/201833381, 1805.02476

Miller N, Fortney JJ (2011) The Heavy-element Masses of Extrasolar Giant Planets, Revealed. ApJ736(2):L29, DOI 10.1088/2041-8205/736/2/L29, 1105.0024

Miotello A, van Dishoeck EF, Kama M, Bruderer S (2016) Determining protoplanetary disk gas masses from CO isotopologues line observations. A&A594:A85, DOI 10.1051/0004-6361/201628159, 1605.07780

Mishenina T, Pignatari M, Côté B, Thielemann FK, Soubiran C, Basak N, Gorbaneva T, Korotin SA, Kovtyukh VV, Wehmeyer B, Bisterzo S, Travaglio C, Gibson BK, Jordan C, Paul A, Ritter C, Herwig F, NuGrid Collaboration (2017) Observing the metal-poor solar neighbourhood: a comparison of galactic chemical evolution predictions*†. MNRAS469(4):4378–4399, DOI 10.1093/\mnras/stx1145, 1705.03642

Mordasini C, Alibert Y, Benz W, Klahr H, Henning T (2012) Extrasolar planet population synthesis . IV. Correlations with disk metallicity, mass, and lifetime. A&A541:A97, DOI 10.1051/0004-6361/201117350, 1201.1036

Mordasini C, Mollière P, Dittkrist KM, Jin S, Alibert Y (2015) Global models of planet formation and evolution. International Journal of Astrobiology 14(2):201–232, DOI 10.1017/S1473550414000263, 1406.5604

Mordasini C, van Boekel R, Mollière P, Henning T, Benneke B (2016) The Imprint of Exoplanet Formation History on Observable Present-day Spectra of Hot Jupiters. ApJ832(1):41, DOI 10.3847/0004-637X/832/1/41, 1609.03019

Mortier A, Santos NC, Sousa SG, Adibekyan VZ, Delgado Mena E, Tsantaki M, Israelian G, Mayor M (2013) New and updated stellar parameters for 71 evolved planet hosts. On the metallicity-giant planet connection. A&A557:A70, DOI 10.1051/0004-6361/201321641, 1307.7870

Muñoz Caro GM, Meierhenrich UJ, Schutte WA, Barbier B, Arcones Segovia A, Rosenbauer H, Thiemann WHP, Brack A, Greenberg JM (2002) Amino acids from ultraviolet irradiation of interstellar ice analogues. Nature416(6879):403–406, DOI 10.1038/416403a

Muzerolle J, Hillenbrand L, Calvet N, Briceño C, Hartmann L (2003) Accretion in Young Stellar/Substellar Objects. ApJ592(1):266–281, DOI 10.1086/375704, astro-ph/0304078

Natta A, Testi L, Muzerolle J, Randich S, Comerón F, Persi P (2004) Accretion in brown dwarfs: An infrared view. A&A424:603–612, DOI 10.1051/0004-6361:20040356, astro-ph/0406106

Nesvorný D (2018) Dynamical Evolution of the Early Solar System. ARA&A56:137–174, DOI 10.1146/annurev-astro-081817-052028, 1807.06647

Nikolaou A, Katyal N, Tosi N, Godolt M, Grenfell JL, Rauer H (2019) What Factors Affect the Duration and Outgassing of the Terrestrial Magma Ocean? ApJ 875(1):11, DOI 10.3847/1538-4357/ab08ed, 1903.07436

Nowak G, Niedzielski A, Wolszczan A, Adamów M, Maciejewski G (2013) BD+15 2940 and HD 233604: Two Giants with Planets Close to the Engulfment Zone. ApJ770(1):53, DOI 10.1088/0004-637X/770/1/53, 1304.6755

Oberg KI, Bergin EA (2020) Astrochemistry and compositions of planetary systems. Physics Reports arXiv:2010.03529, 2010.03529

Öberg KI, Wordsworth R (2019) Jupiter's Composition Suggests its Core Assembled Exterior to the N_2 Snowline. AJ158(5):194, DOI 10.3847/1538-3881/ab46a8, 1909.11246

Öberg KI, Qi C, Fogel JKJ, Bergin EA, Andrews SM, Espaillat C, van Kempen TA, Wilner DJ, Pascucci I (2010) The Disk Imaging Survey of Chemistry with SMA. I. Taurus Protoplanetary Disk Data. ApJ720(1):480–493, DOI 10.1088/0004-637X/720/1/480, 1007.1476

Öberg KI, Qi C, Fogel JKJ, Bergin EA, Andrews SM, Espaillat C, Wilner DJ, Pascucci I, Kastner JH (2011) Disk Imaging Survey of Chemistry with SMA. II. Southern Sky Protoplanetary Disk Data and Full Sample Statistics. ApJ734(2):98, DOI 10.1088/0004-637X/734/2/98, 1104.1236

Öberg KI, Guzmán VV, Furuya K, Qi C, Aikawa Y, Andrews SM, Loomis R, Wilner DJ (2015) The comet-like composition of a protoplanetary disk as revealed by complex cyanides. Nature520(7546):198–201, DOI 10.1038/nature14276, 1505.06347

Öberg KI, Guzmán VV, Merchantz CJ, Qi C, Andrews SM, Cleeves LI, Huang J, Loomis RA, Wilner DJ, Brinch C, Hogerheijde M (2017) H_2CO Distribution and Formation in the TW HYA Disk. ApJ839(1):43, DOI 10.3847/1538-4357/aa689a, 1704.05133

Palme H, Lodders K, Jones A (2014) Solar System Abundances of the Elements. In: Davis AM (ed) Planets, Asteriods, Comets and The Solar System, Volume 2 of Treatise on Geochemistry (Second Edition)., vol 2, Elsevier, pp 15–36

Panić O, Min M (2017) Effects of disc mid-plane evolution on CO snowline location. MNRAS467(1):1175–1185, DOI 10.1093/mnras/stx114, 1703.09708

Panić O, Hogerheijde MR, Wilner D, Qi C (2008) Gas and dust mass in the disc around the Herbig Ae star HD 169142. A&A491(1):219–227, DOI 10.1051/0004-6361:20079261

Papaloizou JCB, Szuszkiewicz E, Terquem C (2018) The TRAPPIST-1 system: orbital evolution, tidal dissipation, formation and habitability. MNRAS476(4):5032–5056, DOI 10.1093/mnras/stx2980, 1711.07932

Pascucci I, Apai D, Luhman K, Henning T, Bouwman J, Meyer MR, Lahuis F, Natta A (2009) The Different Evolution of Gas and Dust in Disks around Sun-Like and Cool Stars. ApJ696(1):143–159, DOI 10.1088/0004-637X/696/1/143, 0810.2552

Pasquini L, Döllinger MP, Weiss A, Girardi L, Chavero C, Hatzes AP, da Silva L, Setiawan J (2007) Evolved stars suggest an external origin of the enhanced metallicity in planet-hosting stars. A&A473:979–982, DOI 10.1051/0004-6361:20077814, 0707.0788

Pegues J, Öberg KI, Bergner JB, Loomis RA, Qi C, Le Gal R, Cleeves LI, Guzmán VV, Huang J, Jørgensen JK, Andrews SM, Blake GA, Carpenter JM, Schwarz KR, Williams JP, Wilner DJ (2020) An ALMA Survey of H_2CO in Protoplanetary Disks. ApJ890(2):142, DOI 10.3847/1538-4357/ab64d9, 2002.12525

Péricaud J, di Folco E, Dutrey A, Augereau JC, Piétu V, Guilloteau S (2016) HD141569A: Disk Dissipation Caught in Action. In: Kastner JH, Stelzer B, Metchev SA (eds) Young Stars & Planets Near the Sun, IAU Symposium, vol 314, pp 201–202, DOI 10.1017/S1743921315006432, `1511.00845`

Perryman M (2018) The Exoplanet Handbook, 2nd edn, Cambridge University Press. DOI 10.1017/9781108304160

Pfeffer J, Kruijssen JMD, Crain RA, Bastian N (2018) The E-MOSAICS project: simulating the formation and co-evolution of galaxies and their star cluster populations. MNRAS475(4):4309–4346, DOI 10.1093/\mnras/stx3124, `1712.00019`

Phuong NT, Chapillon E, Majumdar L, Dutrey A, Guilloteau S, Piétu V, Wakelam V, Diep PN, Tang YW, Beck T, Bary J (2018) First detection of H_2S in a protoplanetary disk. The dense GG Tauri A ring. A&A616:L5, DOI 10.1051/0004-6361/201833766, `1808.00652`

Piersanti L, Straniero O, Cristallo S (2007) A method to derive the absolute composition of the Sun, the solar system, and the stars. A&A462(3):1051–1062, DOI 10.1051/0004-6361:20054505, `astro-ph/0611229`

Piso AMA, Pegues J, Öberg KI (2016) The Role of Ice Compositions for Snowlines and the C/N/O Ratios in Active Disks. ApJ833(2):203, DOI 10.3847/1538-4357/833/2/203, `1611.00741`

Podio L, Kamp I, Codella C, Cabrit S, Nisini B, Dougados C, Sandell G, Williams JP, Testi L, Thi WF, Woitke P, Meijerink R, Spaans M, Aresu G, Ménard F, Pinte C (2013) Water Vapor in the Protoplanetary Disk of DG Tau. ApJ766(1):L5, DOI 10.1088/2041-8205/766/1/L5, `1302.1410`

Podio L, Bacciotti F, Fedele D, Favre C, Codella C, Rygl KLJ, Kamp I, Guidi G, Bianchi E, Ceccarelli C, Coffey D, Garufi A, Testi L (2019) Organic molecules in the protoplanetary disk of DG Tauri revealed by ALMA. A&A623:L6, DOI 10.1051/0004-6361/201834475, `1902.02720`

Podio L, Garufi A, Codella C, Fedele D, Bianchi E, Bacciotti F, Ceccarelli C, Favre C, Mercimek S, Rygl K, Testi L (2020a) ALMA chemical survey of disk-outflow sources in Taurus (ALMA-DOT). II. Vertical stratification of CO, CS, CN, H_2CO, and CH_3OH in a Class I disk. A&A642:L7, DOI 10.1051/0004-6361/202038952, `2008.12648`

Podio L, Garufi A, Codella C, Fedele D, Rygl K, Favre C, Bacciotti F, Bianchi E, Ceccarelli C, Mercimek S, Teague R, Testi L (2020b) ALMA chemical survey of disk-outflow sources in Taurus (ALMA-DOT). III. The interplay between gas and dust in the protoplanetary disk of DG Tau. A&A644:A119, DOI 10.1051/0004-6361/202038600, `2011.01081`

Podolak M, Haghighipour N, Bodenheimer P, Helled R, Podolak E (2020) Detailed Calculations of the Efficiency of Planetesimal Accretion in the Core-accretion Model. ApJ899(1):45, DOI 10.3847/1538-4357/ab9ec1, `1911.12998`

Pollack JB, Hollenbach D, Beckwith S, Simonelli DP, Roush T, Fong W (1994) Composition and Radiative Properties of Grains in Molecular Clouds and Accretion Disks. ApJ421:615, DOI 10.1086/173677

Pollack JB, Hubickyj O, Bodenheimer P, Lissauer JJ, Podolak M, Greenzweig Y (1996) Formation of the Giant Planets by Concurrent Accretion of Solids and Gas. Icarus124(1):62–85, DOI 10.1006/icar.1996.0190

Pontoppidan KM, Blake GA, van Dishoeck EF, Smette A, Ireland MJ, Brown J (2008) Spectroastrometric Imaging of Molecular Gas within Protoplanetary Disk Gaps. ApJ684(2):1323–1329, DOI 10.1086/590400, 0805.3314

Pontoppidan KM, Salyk C, Blake GA, Meijerink R, Carr JS, Najita J (2010) A Spitzer Survey of Mid-infrared Molecular Emission from Protoplanetary Disks. I. Detection Rates. ApJ720(1):887–903, DOI 10.1088/0004-637X/720/1/887, 1006.4189

Poppenhaeger K, Robrade J, Schmitt JHMM (2010) Coronal properties of planet-bearing stars. A&A515:A98, DOI 10.1051/0004-6361/201014245, 1003.5802

Prodanović T, Steigman G, Fields BD (2010) The deuterium abundance in the local interstellar medium. MNRAS406(2):1108–1115, DOI 10.1111/j.1365-2966.2010.16734.x, 0910.4961

Qi C, Öberg KI, Wilner DJ, Rosenfeld KA (2013) First Detection of c-C_3H_2 in a Circumstellar Disk. ApJ765(1):L14, DOI 10.1088/2041-8205/765/1/L14, 1302.0251

Ramírez I, Meléndez J, Asplund M (2009) Accurate abundance patterns of solar twins and analogs. Does the anomalous solar chemical composition come from planet formation? A&A508(1):L17–L20, DOI 10.1051/0004-6361/200913038

Ramírez I, Asplund M, Baumann P, Meléndez J, Bensby T (2010) A possible signature of terrestrial planet formation in the chemical composition of solar analogs. A&A521:A33, DOI 10.1051/0004-6361/201014456, 1008.3161

Ramírez I, Fish JR, Lambert DL, Allende Prieto C (2012) Lithium Abundances in nearby FGK Dwarf and Subgiant Stars: Internal Destruction, Galactic Chemical Evolution, and Exoplanets. ApJ756(1):46, DOI 10.1088/0004-637X/756/1/46, 1207.0499

Ramírez I, Bajkova AT, Bobylev VV, Roederer IU, Lambert DL, Endl M, Cochran WD, MacQueen PJ, Wittenmyer RA (2014) Elemental Abundances of Solar Sibling Candidates. ApJ787(2):154, DOI 10.1088/0004-637X/787/2/154, 1405.1723

Rasio FA, Ford EB (1996) Dynamical instabilities and the formation of extrasolar planetary systems. Science 274:954–956, DOI 10.1126/science.274.5289.954

Reddy BE, Tomkin J, Lambert DL, Allende Prieto C (2003) The chemical compositions of Galactic disc F and G dwarfs. MNRAS340(1):304–340, DOI 10.1046/j.1365-8711.2003.06305.x, astro-ph/0211551

Reddy BE, Lambert DL, Allende Prieto C (2006) Elemental abundance survey of the Galactic thick disc. MNRAS367(4):1329–1366, DOI 10.1111/j.1365-2966.2006.10148.x, astro-ph/0512505

Reffert S, Bergmann C, Quirrenbach A, Trifonov T, Künstler A (2015) Precise radial velocities of giant stars. VII. Occurrence rate of giant extrasolar planets as a function of mass and metallicity. A&A574:A116, DOI

10.1051/0004-6361/201322360, `1412.4634`

Rice WKM, Armitage PJ (2003) On the Formation Timescale and Core Masses of Gas Giant Planets. ApJ598(1):L55–L58, DOI 10.1086/380390, `astro-ph/0310191`

Ritter C, Côté B (2016) NuPyCEE: NuGrid Python Chemical Evolution Environment. `1610.015`

Robinson SE, Laughlin G, Bodenheimer P, Fischer D (2006) Silicon and Nickel Enrichment in Planet Host Stars: Observations and Implications for the Core Accretion Theory of Planet Formation. ApJ643:484–500, DOI 10.1086/502795, `astro-ph/0601656`

Rosotti GP, Dale JE, de Juan Ovelar M, Hubber DA, Kruijssen JMD, Ercolano B, Walch S (2014) Protoplanetary disc evolution affected by star-disc interactions in young stellar clusters. MNRAS441(3):2094–2110, DOI 10.1093/\mnras/stu679, `1404.1931`

Rubin M, Engrand C, Snodgrass C, Weissman P, Altwegg K, Busemann H, Morbidelli A, Mumma M (2020) On the Origin and Evolution of the Material in 67P/Churyumov-Gerasimenko. Space Sci. Rev.216(5):102, DOI 10.1007/s11214-020-00718-2

Ruiz-Lara T, Gallart C, Bernard EJ, Cassisi S (2020) The recurrent impact of the Sagittarius dwarf on the star formation history of the Milky Way. Nature Astronomy 4:965–973, DOI 10.1038/s41550-020-1097-0, `2003.12577`

Sakai N, Sakai T, Hirota T, Watanabe Y, Ceccarelli C, Kahane C, Bottinelli S, Caux E, Demyk K, Vastel C, Coutens A, Taquet V, Ohashi N, Takakuwa S, Yen HW, Aikawa Y, Yamamoto S (2014) Change in the chemical composition of infalling gas forming a disk around a protostar. Nature507(7490):78–80, DOI 10.1038/nature13000

Salyk C, Pontoppidan KM, Blake GA, Najita JR, Carr JS (2011) A Spitzer Survey of Mid-infrared Molecular Emission from Protoplanetary Disks. II. Correlations and Local Thermal Equilibrium Models. ApJ731(2):130, DOI 10.1088/0004-637X/731/2/130, `1104.0948`

Santos NC, Israelian G, Mayor M (2001) The metal-rich nature of stars with planets. A&A373:1019–1031, DOI 10.1051/0004-6361:20010648, `astro-ph/0105216`

Santos NC, Adibekyan V, Figueira P, Andreasen DT, Barros SCC, Delgado-Mena E, Demangeon O, Faria JP, Oshagh M, Sousa SG, Viana PTP, Ferreira ACS (2017) Observational evidence for two distinct giant planet populations. A&A603:A30, DOI 10.1051/0004-6361/201730761, `1705.06090`

Scally A, Clarke C (2001) Destruction of protoplanetary discs in the Orion Nebula Cluster. MNRAS325(2):449–456, DOI 10.1046/j.1365-8711.2001.04274.x, `astro-ph/0012098`

Scandariato G, Maggio A, Lanza AF, Pagano I, Fares R, Shkolnik EL, Bohlender D, Cameron AC, Dieters S, Donati JF, Martínez Fiorenzano AF, Jardine M, Moutou C (2013) A coordinated optical and X-ray spectroscopic campaign on HD 179949: searching for planet-induced chromospheric and coronal activity. A&A552:A7, DOI 10.1051/0004-6361/201219875, `1301.7748`

Schiller M, Bizzarro M, Fernandes VA (2018) Isotopic evolution of the protoplanetary disk and the building blocks of Earth and the Moon. Nature555(7697):507–510, DOI 10.1038/nature25990

Schlaufman KC (2015) A Continuum of Planet Formation between 1 and 4 Earth Radii. ApJ799(2):L26, DOI 10.1088/2041-8205/799/2/L26, 1501. 05953

Schlaufman KC (2018) Evidence of an Upper Bound on the Masses of Planets and Its Implications for Giant Planet Formation. ApJ853:37, DOI 10.3847/1538-4357/aa961c, 1801.06185

Schuler SC, Flateau D, Cunha K, King JR, Ghezzi L, Smith VV (2011) Abundances of Stars with Planets: Trends with Condensation Temperature. ApJ732(1):55, DOI 10.1088/0004-637X/732/1/55, 1103.0757

Schwarz KR, Bergin EA, Cleeves LI, Zhang K, Öberg KI, Blake GA, Anderson D (2018) Unlocking CO Depletion in Protoplanetary Disks. I. The Warm Molecular Layer. ApJ856(1):85, DOI 10.3847/1538-4357/aaae08, 1802.02590

Scott ERD (2007) Chondrites and the Protoplanetary Disk. Annual Review of Earth and Planetary Sciences 35(1):577–620, DOI 10.1146/annurev.earth. 35.031306.140100

Semenov D, Favre C, Fedele D, Guilloteau S, Teague R, Henning T, Dutrey A, Chapillon E, Hersant F, Piétu V (2018) Chemistry in disks. XI. Sulfur-bearing species as tracers of protoplanetary disk physics and chemistry: the DM Tau case. A&A617:A28, DOI 10.1051/0004-6361/201832980, 1806. 07707

Shibata S, Ikoma M (2019) Capture of solids by growing proto-gas giants: effects of gap formation and supply limited growth. MNRAS487(4):4510–4524, DOI 10.1093/\mnras/stz1629, 1906.05530

Shibata S, Helled R, Ikoma M (2020) The origin of the high metallicity of close-in giant exoplanets. Combined effects of resonant and aerodynamic shepherding. A&A633:A33, DOI 10.1051/0004-6361/201936700, 1911.02292

Shkolnik E, Walker GAH, Bohlender DA, Gu PG, Kürster M (2005) Hot Jupiters and Hot Spots: The Short- and Long-Term Chromospheric Activity on Stars with Giant Planets. ApJ622(2):1075–1090, DOI 10.1086/428037, astro-ph/0411655

Shuping RY, Bally J, Morris M, Throop H (2003) Evidence for Grain Growth in the Protostellar Disks of Orion. ApJ587(2):L109–L112, DOI 10.1086/375334

Sing DK (2018) Observational techniques with transiting exoplanetary atmospheres. In: Bozza V, Mancini L, Sozzetti A (eds) Astrophysics of Exoplanetary Atmospheres: 2nd Advanced School on Exoplanetary Science, Springer International Publishing, Cham, pp 3–48, DOI 10.1007/978-3-319-89701-1_1, URL https://doi.org/10.1007/978-3-319-89701-1_1

Sousa SG, Santos NC, Mayor M, Udry S, Casagrande L, Israelian G, Pepe F, Queloz D, Monteiro MJPFG (2008) Spectroscopic parameters for 451 stars in the HARPS GTO planet search program. Stellar [Fe/H] and the frequency of exo-Neptunes. A&A487(1):373–381, DOI 10.1051/0004-6361:200809698,

0805.4826

Tamayo D, Rein H, Petrovich C, Murray N (2017) Convergent Migration Renders TRAPPIST-1 Long-lived. ApJ840(2):L19, DOI 10.3847/2041-8213/aa70ea, 1704.02957

Tanaka H, Takeuchi T, Ward WR (2002) Three-Dimensional Interaction between a Planet and an Isothermal Gaseous Disk. I. Corotation and Lindblad Torques and Planet Migration. ApJ 565(2):1257–1274, DOI 10.1086/324713

Teague R, Henning T, Guilloteau S, Bergin EA, Semenov D, Dutrey A, Flock M, Gorti U, Birnstiel T (2018) Temperature, Mass, and Turbulence: A Spatially Resolved Multiband Non-LTE Analysis of CS in TW Hya. ApJ864(2):133, DOI 10.3847/1538-4357/aad80e, 1808.01768

Terwisscha van Scheltinga J, Hogerheijde MR, Cleeves LI, Loomis RA, Walsh C, Öberg KI, Bergin EA, Bergner JB, Blake GA, Calahan JK, Cazzoletti P, van Dishoeck EF, Guzmán VV, Huang J, Kama M, Qi C, Teague R, Wilner DJ (2021) The TW Hya Rosetta Stone Project. II. Spatially Resolved Emission of Formaldehyde Hints at Low-temperature Gas-phase Formation. ApJ906(2):111, DOI 10.3847/1538-4357/abc9ba, 2011.07073

Thi WF, van Dishoeck EF, Blake GA, van Zadelhoff GJ, Horn J, Becklin EE, Mannings V, Sargent AI, van den Ancker ME, Natta A, Kessler J (2001) H_2 and CO Emission from Disks around T Tauri and Herbig Ae Pre-Main-Sequence Stars and from Debris Disks around Young Stars: Warm and Cold Circumstellar Gas. ApJ561(2):1074–1094, DOI 10.1086/323361, astro-ph/0107006

Thiabaud A, Marboeuf U, Alibert Y, Cabral N, Leya I, Mezger K (2014) From stellar nebula to planets: The refractory components. A&A562:A27, DOI 10.1051/0004-6361/201322208, 1312.3085

Thorngren DP, Fortney JJ, Murray-Clay RA, Lopez ED (2016) The Mass-Metallicity Relation for Giant Planets. ApJ831(1):64, DOI 10.3847/0004-637X/831/1/64, 1511.07854

Throop HB (2011) UV photolysis, organic molecules in young disks, and the origin of meteoritic amino acids. Icarus212(2):885–895, DOI 10.1016/j.\icarus.2011.01.002, 1112.3107

Throop HB, Bally J (2005) Can Photoevaporation Trigger Planetesimal Formation? ApJ623(2):L149–L152, DOI 10.1086/430272, astro-ph/0411647

Timmes FX, Woosley SE, Hartmann DH, Hoffman RD, Weaver TA, Matteucci F (1995a) 26Al and 60Fe from Supernova Explosions. ApJ449:204, DOI 10.1086/176046, astro-ph/9503120

Timmes FX, Woosley SE, Weaver TA (1995b) Galactic Chemical Evolution: Hydrogen through Zinc. ApJS98:617, DOI 10.1086/192172, astro-ph/9411003

Tinetti G, Drossart P, Eccleston P, Hartogh P, Heske A, Leconte J, Micela G, Ollivier M, Pilbratt G, Puig L, Turrini D, Vandenbussche B, Wolkenberg P, Beaulieu JP, Buchave LA, Ferus M, Griffin M, Guedel M, Justtanont K, Lagage PO, Machado P, Malaguti G, Min M, Nørgaard-Nielsen HU, Rataj M, Ray T, Ribas I, Swain M, Szabo R, Werner S, Barstow J, Burleigh M, Cho J, du Foresto VC, Coustenis A, Decin L, Encrenaz T, Galand M, Gillon M,

Helled R, Morales JC, Muñoz AG, Moneti A, Pagano I, Pascale E, Piccioni G, Pinfield D, Sarkar S, Selsis F, Tennyson J, Triaud A, Venot O, Waldmann I, Waltham D, Wright G, Amiaux J, Auguères JL, Berthé M, Bezawada N, Bishop G, Bowles N, Coffey D, Colomé J, Crook M, Crouzet PE, Da Peppo V, Sanz IE, Focardi M, Frericks M, Hunt T, Kohley R, Middleton K, Morgante G, Ottensamer R, Pace E, Pearson C, Stamper R, Symonds K, Rengel M, Renotte E, Ade P, Affer L, Alard C, Allard N, Altieri F, André Y, Arena C, Argyriou I, Aylward A, Baccani C, Bakos G, Banaszkiewicz M, Barlow M, Batista V, Bellucci G, Benatti S, Bernardi P, Bézard B, Blecka M, Bolmont E, Bonfond B, Bonito R, Bonomo AS, Brucato JR, Brun AS, Bryson I, Bujwan W, Casewell S, Charnay B, Pestellini CC, Chen G, Ciaravella A, Claudi R, Clédassou R, Damasso M, Damiano M, Danielski C, Deroo P, Di Giorgio AM, Dominik C, Doublier V, Doyle S, Doyon R, Drummond B, Duong B, Eales S, Edwards B, Farina M, Flaccomio E, Fletcher L, Forget F, Fossey S, Fränz M, Fujii Y, García-Piquer Á, Gear W, Geoffray H, Gérard JC, Gesa L, Gomez H, Graczyk R, Griffith C, Grodent D, Guarcello MG, Gustin J, Hamano K, Hargrave P, Hello Y, Heng K, Herrero E, Hornstrup A, Hubert B, Ida S, Ikoma M, Iro N, Irwin P, Jarchow C, Jaubert J, Jones H, Julien Q, Kameda S, Kerschbaum F, Kervella P, Koskinen T, Krijger M, Krupp N, Lafarga M, Landini F, Lellouch E, Leto G, Luntzer A, Rank-Lüftinger T, Maggio A, Maldonado J, Maillard JP, Mall U, Marquette JB, Mathis S, Maxted P, Matsuo T, Medvedev A, Miguel Y, Minier V, Morello G, Mura A, Narita N, Nascimbeni V, Nguyen Tong N, Noce V, Oliva F, Palle E, Palmer P, Pancrazzi M, Papageorgiou A, Parmentier V, Perger M, Petralia A, Pezzuto S, Pierrehumbert R, Pillitteri I, Piotto G, Pisano G, Prisinzano L, Radioti A, Réess JM, Rezac L, Rocchetto M, Rosich A, Sanna N, Santerne A, Savini G, Scandariato G, Sicardy B, Sierra C, Sindoni G, Skup K, Snellen I, Sobiecki M, Soret L, Sozzetti A, Stiepen A, Strugarek A, Taylor J, Taylor W, Terenzi L, Tessenyi M, Tsiaras A, Tucker C, Valencia D, Vasisht G, Vazan A, Vilardell F, Vinatier S, Viti S, Waters R, Wawer P, Wawrzaszek A, Whitworth A, Yung YL, Yurchenko SN, Osorio MRZ, Zellem R, Zingales T, Zwart F (2018) A chemical survey of exoplanets with ARIEL. Experimental Astronomy 46(1):135–209, DOI 10.1007/s10686-018-9598-x

Trapman L, Miotello A, Kama M, van Dishoeck EF, Bruderer S (2017) Far-infrared HD emission as a measure of protoplanetary disk mass. A&A605:A69, DOI 10.1051/0004-6361/201630308, 1705.07671

Turrini D, Nelson RP, Barbieri M (2015) The role of planetary formation and evolution in shaping the composition of exoplanetary atmospheres. Experimental Astronomy 40(2-3):501–522, DOI 10.1007/s10686-014-9401-6, 1401.5119

Turrini D, Miguel Y, Zingales T, Piccialli A, Helled R, Vazan A, Oliva F, Sindoni G, Panić O, Leconte J, Min M, Pirani S, Selsis F, Coudé du Foresto V, Mura A, Wolkenberg P (2018) The contribution of the ARIEL space mission to the study of planetary formation. Experimental Astronomy 46(1):45–65, DOI 10.1007/s10686-017-9570-1, 1804.06179

Turrini D, Marzari F, Polychroni D, Testi L (2019) Dust-to-gas Ratio Resurgence in Circumstellar Disks Due to the Formation of Giant Planets: The Case of HD 163296. ApJ877(1):50, DOI 10.3847/1538-4357/ab18f5, 1802.04361

Turrini D, Zinzi A, Belinchon JA (2020) Normalized angular momentum deficit: a tool for comparing the violence of the dynamical histories of planetary systems. A&A636:A53, DOI 10.1051/0004-6361/201936301, 2003.05366

Turrini D, Schisano E, Fonte S, Molinari S, Politi R, Fedele D, Panić O, Kama M, Changeat Q, Tinetti G (2021) Tracing the Formation History of Giant Planets in Protoplanetary Disks with Carbon, Oxygen, Nitrogen, and Sulfur. ApJ909(1):40, DOI 10.3847/1538-4357/abd6e5, 2012.14315

Tychoniec Ł, Tobin JJ, Karska A, Chand ler C, Dunham MM, Harris RJ, Kratter KM, Li ZY, Looney LW, Melis C, Pérez LM, Sadavoy SI, Segura-Cox D, van Dishoeck EF (2018) The VLA Nascent Disk and Multiplicity Survey of Perseus Protostars (VANDAM). IV. Free-Free Emission from Protostars: Links to Infrared Properties, Outflow Tracers, and Protostellar Disk Masses. ApJS238(2):19, DOI 10.3847/1538-4365/aaceae, 1806.02434

Udry S, Mayor M, Benz W, Bertaux JL, Bouchy F, Lovis C, Mordasini C, Pepe F, Queloz D, Sivan JP (2006) The HARPS search for southern extra-solar planets. V. A 14 Earth-masses planet orbiting HD 4308. A&A447(1):361–367, DOI 10.1051/0004-6361:20054084, astro-ph/0510354

Valletta C, Helled R (2018) The distribution of heavy-elements in giant protoplanetary atmospheres: the importance of planetesimal-envelope interactions. arXiv e-prints arXiv:1811.10904, 1811.10904

van der Plas G, van den Ancker ME, Acke B, Carmona A, Dominik C, Fedele D, Waters LBFM (2009) Evidence for CO depletion in the inner regions of gas-rich protoplanetary disks. A&A500(3):1137–1141, DOI 10.1051/0004-6361/200811148, 0810.3417

van Dishoeck EF, Kristensen LE, the WISH Team (2021) Water in star-forming regions (WISH): Physics and chemistry from clouds to disks as probed by Herschel spectroscopy. arXiv e-prints arXiv:2102.02225, 2102.02225

van 't Hoff MLR, Tobin JJ, Trapman L, Harsono D, Sheehan PD, Fischer WJ, Megeath ST, van Dishoeck EF (2018) Methanol and its Relation to the Water Snowline in the Disk around the Young Outbursting Star V883 Ori. ApJ864(1):L23, DOI 10.3847/2041-8213/aadb8a, 1808.08258

van't Hoff MLR, Harsono D, Tobin JJ, Bosman AD, van Dishoeck EF, Jørgensen JK, Miotello A, Murillo NM, Walsh C (2020) Temperature Structures of Embedded Disks: Young Disks in Taurus Are Warm. ApJ901(2):166, DOI 10.3847/1538-4357/abb1a2

Vazan A, Helled R (2020) Explaining the low luminosity of Uranus: a self-consistent thermal and structural evolution. A&A633:A50, DOI 10.1051/0004-6361/201936588, 1908.10682

Vazan A, Helled R, Kovetz A, Podolak M (2015) Convection and Mixing in Giant Planet Evolution. ApJ803:32, DOI 10.1088/0004-637X/803/1/32,

1502.03270

Vazan A, Helled R, Podolak M, Kovetz A (2016) The Evolution and Internal Structure of Jupiter and Saturn with Compositional Gradients. ApJ829:118, DOI 10.3847/0004-637X/829/2/118, 1606.01558

Vazan A, Helled R, Guillot T (2018) Jupiter's evolution with primordial composition gradients. A&A610:L14, DOI 10.1051/0004-6361/201732522, 1801.08149

Villenave M, Ménard F, Dent WRF, Duchêne G, Stapelfeldt KR, Benisty M, Boehler Y, van der Plas G, Pinte C, Telkamp Z, Wolff S, Flores C, Lesur G, Louvet F, Riols A, Dougados C, Williams H, Padgett D (2020) Observations of edge-on protoplanetary disks with ALMA. I. Results from continuum data. A&A642:A164, DOI 10.1051/0004-6361/202038087, 2008.06518

Wakeford HR, Sing DK, Kataria T, Deming D, Nikolov N, Lopez ED, Tremblin P, Amundsen DS, Lewis NK, Mandell AM, Fortney JJ, Knutson H, Benneke B, Evans TM (2017) HAT-P-26b: A Neptune-mass exoplanet with a well-constrained heavy element abundance. Science 356(6338):628–631, DOI 10.1126/science.aah4668, 1705.04354

Walker GAH, Croll B, Matthews JM, Kuschnig R, Huber D, Weiss WW, Shkolnik E, Rucinski SM, Guenther DB, Moffat AFJ, Sasselov D (2008) MOST detects variability on τ Bootis A possibly induced by its planetary companion. A&A482(2):691–697, DOI 10.1051/0004-6361:20078952, 0802.2732

Walsh C, Millar TJ, Nomura H, Herbst E, Widicus Weaver S, Aikawa Y, Laas JC, Vasyunin AI (2014) Complex organic molecules in protoplanetary disks. A&A563:A33, DOI 10.1051/0004-6361/201322446, 1403.0390

Walsh C, Nomura H, van Dishoeck E (2015) The molecular composition of the planet-forming regions of protoplanetary disks across the luminosity regime. A&A582:A88, DOI 10.1051/0004-6361/201526751, 1507.08544

Walsh C, Loomis RA, Öberg KI, Kama M, van 't Hoff MLR, Millar TJ, Aikawa Y, Herbst E, Widicus Weaver SL, Nomura H (2016) First Detection of Gas-phase Methanol in a Protoplanetary Disk. ApJ823(1):L10, DOI 10.3847/2041-8205/823/1/L10, 1606.06492

Weidenschilling SJ, Marzari F (1996) Gravitational scattering as a possible origin for giant planets at small stellar distances. Nature384(6610):619–621, DOI 10.1038/384619a0

Willacy K, Woods PM (2009) Deuterium Chemistry in Protoplanetary Disks. II. The Inner 30 AU. ApJ703(1):479–499, DOI 10.1088/0004-637X/703/1/479, 0908.1114

Wilson RF, Teske J, Majewski SR, Cunha K, Smith V, Souto D, Bender C, Mahadevan S, Troup N, Allende Prieto C, Stassun KG, Skrutskie MF, Almeida A, García-Hernández DA, Zamora O, Brinkmann J (2018) Elemental Abundances of Kepler Objects of Interest in APOGEE. I. Two Distinct Orbital Period Regimes Inferred from Host Star Iron Abundances. AJ155(2):68, DOI 10.3847/1538-3881/aa9f27, 1712.01198

Winter AJ, Booth RA, Clarke CJ (2018a) Evidence of a past disc-disc encounter: HV and DO Tau. MNRAS479(4):5522–5531, DOI 10.1093/\mnras/

sty1866, 1807.04295

Winter AJ, Clarke CJ, Rosotti G, Ih J, Facchini S, Haworth TJ (2018b) Protoplanetary disc truncation mechanisms in stellar clusters: comparing external photoevaporation and tidal encounters. MNRAS478(2):2700–2722, DOI 10.1093/\mnras/sty984, 1804.00013

Winter AJ, Kruijssen JMD, Chevance M, Keller BW, Longmore SN (2020a) Prevalent externally driven protoplanetary disc dispersal as a function of the galactic environment. MNRAS491(1):903–922, DOI 10.1093/\mnras/stz2747, 1907.04602

Winter AJ, Kruijssen JMD, Longmore SN, Chevance M (2020b) Stellar clustering shapes the architecture of planetary systems. Nature586(7830):528–532, DOI 10.1038/s41586-020-2800-0, 2010.10531

Woitke P, Thi WF, Kamp I, Hogerheijde MR (2009) Hot and cool water in Herbig Ae protoplanetary disks. A challenge for Herschel. A&A501(1):L5–L8, DOI 10.1051/0004-6361/200912249, 0906.0448

Woitke P, Min M, Pinte C, Thi WF, Kamp I, Rab C, Anthonioz F, Antonellini S, Baldovin-Saavedra C, Carmona A, Dominik C, Dionatos O, Greaves J, Güdel M, Ilee JD, Liebhart A, Ménard F, Rigon L, Waters LBFM, Aresu G, Meijerink R, Spaans M (2016) Consistent dust and gas models for protoplanetary disks. I. Disk shape, dust settling, opacities, and PAHs. A&A586:A103, DOI 10.1051/0004-6361/201526538, 1511.03431

Wolszczan A, Frail DA (1992) A planetary system around the millisecond pulsar PSR1257 + 12. Nature355(6356):145–147, DOI 10.1038/355145a0

Zhang K, Bergin EA, Blake GA, Cleeves LI, Schwarz KR (2017) Mass inventory of the giant-planet formation zone in a solar nebula analogue. Nature Astronomy 1:0130, DOI 10.1038/s41550-017-0130, 1705.04746

Zhu Z, Zhang S, Jiang YF, Kataoka A, Birnstiel T, Dullemond CP, Andrews SM, Huang J, Pérez LM, Carpenter JM, Bai XN, Wilner DJ, Ricci L (2019) One Solution to the Mass Budget Problem for Planet Formation: Optically Thick Disks with Dust Scattering. ApJ877(2):L18, DOI 10.3847/2041-8213/ab1f8c, 1904.02127

Zingales T, Tinetti G, Pillitteri I, Leconte J, Micela G, Sarkar S (2018) The ARIEL mission reference sample. Experimental Astronomy 46(1):67–100, DOI 10.1007/s10686-018-9572-7, 1706.08444

Zinzi A, Turrini D (2017) Anti-correlation between multiplicity and orbital properties in exoplanetary systems as a possible record of their dynamical histories. A&A605:L4, DOI 10.1051/0004-6361/201731595, 1709.00003